University of Reading

Endothelium-mediated regulation of platelet activation: involvement of multiple protein kinases

Article

Published Version

Creative Commons: Attribution 4.0 (CC-BY)

Open Access

Provenzale, I., Solari, F. A., Schonichen, C., Brouns, S. L.N., Fernandez, D. I., Kuijpers, M. J.E., Van der Meijden, P. E.J., Gibbins, J. M. ORCID: https://orcid.org/0000-0002-0372-5352, Sickman, A., Jones, C. ORCID: https://orcid.org/0000-0001-7537-1509 and Heemskerk, J. W.M. (2024) Endothelium-mediated regulation of platelet activation: involvement of multiple protein kinases. FASEB Journal, 38 (4). e23468. ISSN 0892-6638 doi: https://doi.org/10.1096/fj.202300360RR Available at https://centaur.reading.ac.uk/115200/

It is advisable to refer to the publisher's version if you intend to cite from the work. See Guidance on citing.

To link to this article DOI: http://dx.doi.org/10.1096/fj.202300360RR

Publisher: Federation of American Societies for Experimental Biology

All outputs in CentAUR are protected by Intellectual Property Rights law, including copyright law. Copyright and IPR is retained by the creators or other copyright holders. Terms and conditions for use of this material are defined in the End User Agreement.

University of Reading

www.reading.ac.uk/centaur

CentAUR

Central Archive at the University of Reading

Reading's research outputs online

Check for updates

Received: 25 February 2023 | Revised: 11 January 2024 | Accepted: 23 January 2024

DOI: 10.1096/fj.202300360RR

RESEARCH ARTICLE

The FASEB Journal

Endothelium-mediated regulation of platelet activation: Involvement of multiple protein kinases

Isabella Provenzale[1,2,3] | **Fiorella A. Solari**[3] | **Claudia Schönichen**[1,4] | **Sanne L. N. Brouns**[1] | **Delia I. Fernández**[1,5] | **Marijke J. E. Kuijpers**[1,6] | **Paola E. J. van der Meijden**[1,6] | **Jonathan M. Gibbins**[2] | **Albert Sickmann**[3,7,8] | **Chris Jones**[2] | **Johan W. M. Heemskerk**[1,9]

[1]Department of Biochemistry, Cardiovascular Research Institute Maastricht (CARIM), Maastricht University, Maastricht, The Netherlands

[2]Institute for Cardiovascular and Metabolic Research (ICMR), School of Biological Sciences, University of Reading, Reading, UK

[3]Leibniz-Institut für Analytische Wissenschaften – ISAS – e.V., Dortmund, Germany

[4]Center for Thrombosis and Haemostasis, University Medical Center of the Johannes Gutenberg University Mainz, Mainz, Germany

[5]Center for Research in Molecular Medicine and Chronic Diseases (CIMUS), Universidade de Santiago de Compostela, Santiago de Compostela, Spain

[6]Thrombosis Expertise Center, Heart and Vascular Center, Maastricht University Medical Center+, Maastricht, The Netherlands

[7]Medizinische Fakultät, Medizinische Proteom-Center, Ruhr-Universität Bochum, Bochum, Germany

[8]Department of Chemistry, College of Physical Sciences, University of Aberdeen, Aberdeen, UK

[9]Synapse Research Institute Maastricht, Maastricht, The Netherlands

Correspondence
Claudia Schönichen, Department of Biochemistry, Cardiovascular Research Institute Maastricht (CARIM), Maastricht University, Maastricht, The Netherlands.
Email: c.schonichen@maastrichtuniversity.nl

Abstract

The endothelial regulation of platelet activity is incompletely understood. Here we describe novel approaches to find molecular pathways implicated on the platelet–endothelium interaction. Using high-shear whole-blood microfluidics, employing coagulant or non-coagulant conditions at physiological temperature, we observed that the presence of human umbilical vein endothelial cells (HUVEC) strongly suppressed platelet adhesion and activation, via the collagen

Abbreviations: ACD, acid citrate dextrose; ADP, adenosine diposphate; AKT, Rac serine/threonine kinases; ANOVA, analysis of variance; BCA, bicinchoninic acid assay; BSA, bovine serum albumin; BTK, bruton tyrosine kinase; CAMK, Ca^{2+}/calmodulin-dependent protein kinase; CAMP, calmodulin-dependent kinases; CDK, cyclin-dependent kinase; CLK, dual specificity protein kinase; CRP-XL, collagen-related peptide, cross-linked; DYRK, dual-specificity tyrosine-regulated kinases; EPCR, endothelial protein C receptor; FDR, false discovery rate; GPVI, glycoprotein VI; HUVEC, human umbilical vein endothelial cells; IMAC, immobilized metal affinity chromatography; KEGG, Kyoto Encyclopedia of Genes and Genomes; KSEA, Kinase-Substrate Enrichment Analysis; LC, liquid chromatography; L-NNA, Nω-nitro-l-arginine; log2 FC, log2 fold change; MAPK, mitogen-activated protein kinases; MS, mass spectrometry; NAV, normalized abundance value; NO, nitric oxide; PAR, protease-activated receptor; PBS, phosphate buffered saline; PCK, protein kinase C; PCKA, protein kinase A; PKA, protein kinase A; PKC, protein kinase C; PKG, protein kinase G; PRKACA, protein kinase CAMP-activated catalytic subunit alpha; PRKACB, protein kinase CAMP-activated catalytic subunit beta; PRKCD, protein kinase C delta; PRKCQ, protein kinase C theta; PRP, platelet-rich plasma; PSM, peptide spectra matches; RFU, relative fluorescent unit; SAC, surface area coverage; SD, standard deviation; SDS, Sodium dodecyl sulfate; SRC, proto-oncogene tyrosine-protein kinase Src; STK, serine-threonine kinases; SYK, tyrosine-protein kinase SYK; TF, tissue factor; TMT, tandem mass tag; VOAC, vessel-on-a-chip; VWF, von Willebrandt factor.

Isabella Provenzale, Fiorella A. Solari, and Claudia Schönichen contributed equally to this study.

This is an open access article under the terms of the Creative Commons Attribution License, which permits use, distribution and reproduction in any medium, provided the original work is properly cited.
© 2024 The Authors. *The FASEB Journal* published by Wiley Periodicals LLC on behalf of Federation of American Societies for Experimental Biology.

Funding information
EC | Horizon 2020 Framework Programme (H2020), Grant/Award Number: 766118 and 813409

receptor glycoprotein VI (GPVI) and the PAR receptors for thrombin. Real-time monitoring of the cytosolic Ca^{2+} rises in the platelets indicated no major improvement of inhibition by prostacyclin or nitric oxide. Similarly under stasis, exposure of isolated platelets to HUVEC reduced the Ca^{2+} responses by collagen-related peptide (CRP-XL, GPVI agonist) and thrombin (PAR agonist). We then analyzed the label-free phosphoproteome of platelets (three donors), exposed to HUVEC, CRP-XL, and/or thrombin. High-resolution mass spectrometry gave 5463 phosphopeptides, corresponding to 1472 proteins, with good correlation between biological and technical replicates ($R > .86$). Stringent filtering steps revealed 26 regulatory pathways (Reactome) and 143 regulated kinase substrates (PhosphoSitePlus), giving a set of protein phosphorylation sites that was differentially (44) or similarly (110) regulated by HUVEC or agonist exposure. The differential regulation was confirmed by stable-isotope analysis of platelets from two additional donors. Substrate analysis indicated major roles of poorly studied protein kinase classes (MAPK, CDK, DYRK, STK, PKC members). Collectively, these results reveal a resetting of the protein phosphorylation profile in platelets exposed to endothelium or to conventional agonists and to endothelium-promoted activity of a multi-kinase network, beyond classical prostacyclin and nitric oxide actors, that may contribute to platelet inhibition.

KEYWORDS
endothelial cells, glycoprotein VI, inter-cellular cross-talk, phosphoproteome, platelets, protease-activated receptors

1 | INTRODUCTION

Fundamental in the current understanding of controlled hemostasis is that the endothelium suppresses the activation of flowing blood platelets and the coagulation system.[1,2] Under physiological conditions with an undamaged, non-inflamed endothelium, the endothelial surface membrane and endothelium-derived mediators are considered to prevent platelets from local adhesion and activation. Distortion or inflammation of an endothelium can induce platelet activation and clot formation and hence a hemostatic or thrombotic response. So far, a limited number of anti-hemostatic endothelial mediators have been identified. Established mediators are (i) release products such as prostacyclin, other prostanoids and nitric oxide, which in platelets elevate the cyclic nucleotides, cAMP and cGMP[3–5]; (ii) the surface ectonucleotidase complex of CD39 and CD73, which degrades adenosine nucleotides into platelet-inhibiting adenosine[6]; (iii) endothelins with an incompletely understood mode of action[7]; and (iv) heparin-like proteoglycans of the glycocalyx.[2] Concerning coagulation management, (v) endothelial cells additionally stimulate anticoagulant pathways via the protein C receptor (EPCR), thrombomodulin, and tissue-factor pathway inhibitor.[2,8] To which extent these and other mediators control platelet activation processes is incompletely understood. Here, we used several approaches, including microfluidics, platelet Ca^{2+} monitoring, and phospho-proteomic analyses, to study the endothelial effects on platelets.

Recent microfluidic studies, in which an endothelial monolayer is exposed to flowing blood, provided first insight how endothelial cells act to control of the activation of platelets and coagulation.[9] It was shown, using a micro-engineered endothelialized microfluidic model for bleeding, that a pressure-induced loss of endothelial cells induced local platelet activation and thrombus formation, with a particular role of procoagulant cells near the site of the injury.[10] Tissue factor (TF) present underneath the distorted endothelial cells triggered local clot formation. In microfluidic channels covered with collagen and human umbilical vein endothelial cells (HUVEC), the presence of collagen appeared to be necessary for the restriction of neutrophil transmigration.[11] In another vessel-on-a-chip (VOAC) model, microchannels were co-coated with collagen and TF and then overgrown by HUVEC until subconfluence.[12] The presence of endothelial cells resulted in potent anti-platelet and anti-coagulant properties, which

15306860, 2024, 4, Downloaded from https://faseb.onlinelibrary.wiley.com/doi/10.1096/fj.202300360RR by Test, Wiley Online Library on [12/02/2024]. See the Terms and Conditions (https://onlinelibrary.wiley.com/terms-and-conditions) on Wiley Online Library for rules of use; OA articles are governed by the applicable Creative Commons License

in part were mediated by surface-expressed thrombomodulin and the glycocalyx. Herein, the HUVEC—although not vascular-bed-specific cells—acted in a consistent way when used at low passage numbers. Accordingly, such microfluidic VOAC models containing collagen, TF, and endothelial cells can provide valuable information on regulatory mechanisms of hemostasis and thrombosis.

Platelet exposure to collagens and to thrombin (formed upon coagulation) results in activation via glycoprotein VI (GPVI) and the protease-activated receptors PAR1/4, respectively. Agonists of both receptor types induce rises in cytosolic $[Ca^{2+}]_i$, followed by a multitude of responses, including platelet adhesion, shape change, secretion, integrin αIIbβ3 activation, aggregation, and procoagulant activity.[2,5,13,14] It is commonly considered that endothelial-released prostacyclin (stable analog iloprost) and nitric oxide suppress the majority of these platelet activation responses, acting through broad-spectrum cAMP-dependent protein kinase A (PKA) and cGMP-dependent protein kinase G (PKG), respectively.[3,4,15] A crucial step in this suppression is provided by PKA- and PKG-dependent downregulation of the platelet $[Ca^{2+}]_i$ rises.[2,14] Accordingly, PKA and PKG are supposed to be the main kinases, by which the endothelial mediators suppress platelet functions.

Indeed, analysis of the phosphoproteome of platelets has pointed to a PKA- and PKG-dependent modulation of the protein phosphorylation status. Thus, incubation of platelets with the prostacyclin analogue iloprost causes phosphorylation changes in multiple proteins,[16] of which number was even increased, when the platelets were consecutively stimulated with ADP.[17] Similarly, platelet incubation with a nitric oxide-releasing compound, acting via PKG, resulted in substantial phosphorylation changes.[18] However, to which extent these changes correspond to endothelial effects on platelets has not been determined so far.

In this paper, we used an improved microfluidic method to investigate how the presence of HUVEC affects platelet activation induced by GPVI or PAR1/4 receptors. This method allowed real-time monitoring of platelet responses during whole-blood perfusion over endothelial cells at high shear rate and 37°C. Based on the observed inhibitory effects of HUVEC, we determined the changes by endothelium exposure in the phosphoproteome of platelets. For this purpose, we used a sensitive label-free phosphoproteome analysis, firstly applied to platelets, which was validated by conventional stable-isotope phosphoprotein analysis. The combination of an improved microfluidic VOAC approach combined with extensive phosphorylation analysis revealed a network of regulatory protein kinases, extending from PKA and PKG, that was differentially modulated by HUVEC, GPVI, and PAR1/4 receptors.

2 | MATERIALS AND METHODS

2.1 | Blood collection

Human blood was collected from healthy volunteers, after full informed consent according to the declaration of Helsinki. Venous blood was collected into 3.2% trisodium citrate Vacuette tubes (Greiner Bio-One, Alphen a/d Rijn, The Netherlands). Approval was obtained from the local Medical Ethics Committee. All donors were healthy subjects in the age range of 18–60 years, not taking antiplatelet medication for at least 2 weeks, and with normal counts of platelets ($255–328 \times 10^9$/L) and red blood cell ($3.86–4.20 \times 10^{12}$/L). All blood samples were checked for the absence of clotting. Control tests confirmed a normal platelet aggregation. According to the ethical approval, person-identifiable characteristics of the blood donors were not revealed. Citrated blood samples were used for flow studies and in parallel for the isolation of platelets.

2.2 | Endothelial cell culture

Human umbilical vein endothelial cells (PromoCell, Heidelberg, Germany) of passages 4–6 were cultured on flasks coated with rat tail collagen (35.5 μg/mL, EMD Millipore, Darmstadt, Germany) in regular endothelial cell growth medium (PromoCell C-22010), supplemented with growth medium supplement mix (PromoCell C-39215), 1% penicillin/streptomycin (Gibco, Waltham, MA, USA), and 1% L-glutamine (Gibco), using procedures described before.[19] For flow-based studies, about 500 000 of the cultured cells were seeded on a collagen I-coated (50 μg/mL, Nycomed, Hoofddorp, The Netherlands) sterile Menzel glass coverslip (24 × 60 mm, Thermo-Fisher), whether or not post-coated with TF (500 pM, Dade-Behring, Breda, The Netherlands), and grown until sub-confluency in the same medium. For static studies, the HUVEC were seeded on collagen-coated 12-well plates, coated with rat tail collagen and grown in the same medium. The culturing was stopped when the cells were confluent and showed a cobblestone morphology. All HUVEC culturing was at 37°C in an atmosphere containing 5% CO_2.[19]

2.3 | Post-fixation staining of endothelial cells on coverslips

If required, cultured HUVEC on coverslips were fixed with 4% paraformaldehyde, followed by permeabilization with 0.005% sodium dodecyl sulfate (SDS) in phosphate-buffered saline (PBS). After washing with PBS and blocking with PBS plus 5% bovine serine albumin (BSA), the

15306860, 2024, 4, Downloaded from https://faseb.onlinelibrary.wiley.com/doi/10.1096/fj.202300360RR by Test, Wiley Online Library on [12/02/2024]. See the Terms and Conditions (https://onlinelibrary.wiley.com/terms-and-conditions) on Wiley Online Library for rules of use; OA articles are governed by the applicable Creative Commons License

cells were incubated with primary rabbit anti-human VWF Ab (1:100, Dako, Amstelveen, The Netherlands) overnight at 4°C. This was followed by a 1-h incubation with secondary Alexa Fluor (AF)647 labeled goat, anti-rabbit Ab (1:400, A-21245, Thermo-Fisher Scientific, Eindhoven, The Netherlands) in combination with Oregon Green(OG)488 labeled phalloidin (1:100, Thermo-Fisher Scientific). Finally, the cells were post-stained for 10 min with the nuclear dye Hoechst 33342 (1 μg/mL, Molecular Probes, Waltham, MA, USA). Multicolor confocal images were captured with a Zeiss LSM7 confocal microscope (Carl Zeiss, Oberkochen, Germany), following settings as described previously.[20]

Where indicated, the HUVEC on coverslips—immediately before and during blood perfusion—were treated with Nω-nitro-l-arginine (L-NNA, 100 μM, Cayman Chemicals, Ann Harbor, USA), acetylsalicylic acid (aspirin 100 μM, Sanofi, France), ecto-ATPase (CD39) inhibitor ARL-67156 (100 μM, Santa Cruz Biotechnology, Heidelberg, Germany), or heparinase III (500 mU/mL, Merck, Darmstadt, Germany). The expression of NOS1/3 and PTGS1/2 in the batch of HUVEC was confirmed on the transcript level.

2.4 | Platelet isolation and loading with Ca^{2+} dyes

Human platelet-rich plasma (PRP) and washed platelets were obtained from citrated blood samples by centrifugation in the presence of 10 vol% of ACD (acid citrate dextrose, 85 mM sodium citrate, 78 mM citric acid, 11 mM glucose) and a wash with Hepes buffer pH 6.6 (136 mM NaCl, 10 mM Hepes, 2.7 mM KCl, 2 mM $MgCl_2$, 1 mg/mL glucose, 1 mg/mL bovine serum albumin, BSA), similarly as before.[21] After washing, the platelet pellets were resuspended in Hepes buffer, pH 7.45 (136 mM NaCl, 10 mM Hepes, 2.7 mM KCl, 2 mM $MgCl_2$, 1 mg/mL glucose, 1 mg/mL bovine serum albumin) in the presence of 0.2 units/mL apyrase at a concentration of 2×10^8/mL.

For measurements of cytosolic $[Ca^{2+}]_i$ under flow, washed platelets were loaded with 8 μM Fluo-4 acetoxymethyl ester and pluronic (0.4 mg/mL) (Thermo-Fisher Scientific) for 40 min at 37°C.[22] After loading, the cells were centrifuged in the presence of 10% vol ACD and apyrase and then resuspended into Hepes buffer pH 7.45. Platelet count was measured using a Sysmex-XP300 hematology analyzer (Pineville, NC, USA). The Fluo-4-loaded platelets were reconstituted with samples of autologous blood at 30% of total count. Fluo-4 was used as a Ca^{2+}-stain in this case, because of its suitability for capturing platelet Ca^{2+} responses in whole-blood perfusion.

For separate measurements of cytosolic $[Ca^{2+}]_i$ in stasis, washed platelets were loaded at 1:1 vol/vol with the dye Calcium-6 for 120 min at 37°C, following the manufacturer's instructions (Calcium-6 Assay Kit from Molecular Devices, San Jose, CA, USA). This Calcium-6 staining procedure allowed to measure platelet $[Ca^{2+}]_i$ rises in 96-well plates without extra centrifugation step.[23]

2.5 | Microfluidic experiments with platelets exposed to endothelial cells in flowing whole blood

For studying the exposure of platelets in whole-blood to endothelial cells under flow conditions, we adapted a previous microfluidic method, where HUVEC were grown until sub-confluency on a collagen and TF matrix.[12] We changed the earlier used 200 μm deep Ibidi μ-luer slides,[12] as these did not allow real-time observations of platelets under high shear. Key adaptations made were as follows: (i) incorporation of HUVEC in the shallow parallel-plate Maastricht flow chamber (50 μm depth × 3 mm width × 20 mm length)[2]; (ii) blood flow at physiological temperature of 37°C with a chamber built around the confocal microscope. In brief, washed glass coverslips (24 × 60 mm, Menzel) were coated with collagen-I (50 μg/mL, Nycomed, Hoofddorp, The Netherlands) and in part post-coated with TF (500 pM, Dade-Behring, Breda, The Netherlands) under sterile conditions. HUVEC (~500 000 cells, passage 4–6) were seeded on the coated coverslips and then cultured until a partial surface area coverage of 50%–60% cells was reached. Control glass coverslips were treated similarly, but using vehicle buffer instead of HUVEC. On the day of experimentation, the HUVEC were stained with vital nuclear dye Hoechst 33342 (1 μg/mL, Thermo-Fisher) in growth medium for 10 min at 37°C. Subsequently, HUVEC-containing or control coverslips were mounted onto the microfluidic chamber and used for whole blood perfusion at 37°C.

For non-coagulant perfusion experiments, 500 μL samples of citrated blood (temperature adapted) were treated with thrombin inhibitor PPACK (40 μM, f.c., Bachem, Bubendorf, Switzerland) and recalcified with cation mixture (3.75 mM $MgCl_2$ and 7.5 mM $CaCl_2$, f.c.). For experiments incorporating coagulation, 500 μL blood was recalcified during flow using a Y-shaped tubing system and two pulse-free perfusion pumps, which allowed complete mixing of the blood with recalcification medium, at volume ratio of 10:1, respectively.[24] In contrast to the earlier method,[12] blood samples were flowed at an arterial shear rate of 1000 s^{-1}, over a time

15306860, 2024, 4, Downloaded from https://faseb.onlinelibrary.wiley.com/doi/10.1096/fj.202300360RR by Test, Wiley Online Library on [12/02/2024]. See the Terms and Conditions (https://onlinelibrary.wiley.com/terms-and-conditions) on Wiley Online Library for rules of use; OA articles are governed by the applicable Creative Commons License

period >3.5 min at 37°C, with chamber and perfusion pumps placed in the temperature chamber. Where indicated, blood samples were spiked with autologous Fluo-4-loaded platelets (30% of platelet count) and AF647-labeled fibrinogen (5 μg/mL, Invitrogen Life Technologies, Waltham, MA, USA).

During whole blood perfusion (37°C), multicolor confocal time series (interval 1 s, 200 cycles) were captured in real time with a line-scanning Zeiss LSM7 microscope (Jena, Germany) operating at high speed, equipped with 488, 532, 647 nm lasers and a 63×/1.4 numerical aperture oil immersion objective (Carl Zeiss, Oberkochen, Germany).[25] This imaging frequency allowed to discriminate between adhesion and activation of the Fluo-4-loaded platelets,[26] and precise detection of the fibrin formation.[27] Time series of fluorescence images were analyzed for changes in fluorescence intensity and for platelet adhesion, using Fiji/ImageJ software. During and after blood flow, brightfield microscopic images were taken to check for intactness of the endothelial cells.[20] Where indicated, HUVEC-containing coverslips were fixed post-perfusion, and stained for actin and nuclei.

2.6 | Experiments with platelets exposed to endothelial cells under stasis

For static experiments, confluent HUVEC in 12-well plates with 1.5 mL growth medium were rinsed twice with sterile phosphate-buffered saline. Control wells not containing HUVEC were treated similarly. After careful removal of the saline, a suspension of Calcium-6-loaded platelets in Hepes buffer pH 7.45 was added to each well (3×10^8 in 1.5 mL). After 30 min of incubation, the platelet suspension was recollected, and immediately transferred to and aliquoted over a 96-well plate for real-time measurements of $[Ca^{2+}]_i$. Platelet Ca^{2+} responses were semi-automatically measured (1 mM $CaCl_2$ present) in a FlexStation 3 robot (Molecular Devices) at 37°C for up to 60 min, as described.[23] In brief, 200 μL of Calcium-6-loaded platelets per well were stimulated by automated pipetting with 20 μL of agonist solution. Agonists were cross-linked collagen related peptide (CRP-XL, 10 μg/mL; CambCol Laboratories; Cambridge, UK) and human α-thrombin (4 nM; Sigma-Aldrich, Zwijndrecht, The Netherlands).[28] The final platelet count was 2×10^8/mL. The injection speed of agonist solution was set at 125 μL/s, as required for complete mixing at a diffusion-limited time.[29] Fluorescence measurements were performed per well-plate row at single excitation wavelength of 485 nm.[29]

2.7 | Platelet preparation for proteome analysis

For proteomic analyses, platelets from three healthy donors (D1-3) were exposed to HUVEC, and then recollected and activated. The platelets in Hepes buffer pH 7.45 (5.0×10^8/mL) were exposed for 30 min to HUVEC, grown to confluency in 12-well plates at 37°C. Parallel control platelet samples were incubated in control wells not containing HUVEC, but otherwise treated similarly. After 30 min, the platelet suspensions were carefully recollected in Eppendorf tubes and immediately incubated with vehicle medium or agonist solution, i.e., CRP-XL (10 μg/mL) or α-thrombin (4 nM) in the presence of 1 mM $CaCl_2$, for indicated times. Incubations were performed in parallel to experiments to measure platelet $[Ca^{2+}]_i$. For proteomics, platelet reactions were stopped by adding per tube 1 volume of lysis buffer (50 mM Tris, 1% SDS, 150 mM NaCl, 1 tablet PhosSTOP/7 mL, pH 7.8).[15] Lysed samples were immediately frozen and stored at −80°C until further processing.

2.8 | Sample workup for establishing proteomes

For platelet analysis by mass spectrometry, procedures were used as before,[17,30] but with key modifications to obtain label-free proteomes and phospho-proteomes.[31] Protein concentrations of lysed platelet samples were measured using a bicinchoninic acid protein assay kit (Thermo Scientific-Pierce, Bremen, Germany). Then, subsamples containing 100 μg of proteins were stored for further workup. Cysteines were reduced with 10 mM dithiothreitol (30 min at 56°C), and free sulfhydryl groups were alkylated with 30 mM iodoacetamide (30 min at room temperature in the dark). After dilution in ice-cold ethanol (1:10), the protein samples were incubated at high throughput for 1 h at −40°C, centrifuged at 20000 *g* for 30 min (4°C), and supernatants were carefully removed. The supernatants were subjected to an additional precipitation step by addition of 200 μL ice-cold acetone (30 min) and centrifugation. The combined precipitated proteins were solubilized into 6 M urea and digested using trypsin (sequencing-grade modified trypsin, Promega, Madison, WI, USA at a 1:20 enzyme: protein ratio) in the presence of 2 mM $CaCl_2$ and 50 mM NH_4HCO_3. To allow trypsinization, the protein samples were incubated at high throughput for 18 h at 37°C, after which digestion was halted by addition of 1% trifluoroacetic acid. Digests were dried under vacuum and then resuspended in 0.1% trifluoroacetic acid. After transferring to

15306860, 2024, 4, Downloaded from https://faseb.onlinelibrary.wiley.com/doi/10.1096/fj.202300360RR by Test, Wiley Online Library on [12/02/2024]. See the Terms and Conditions (https://onlinelibrary.wiley.com/terms-and-conditions) on Wiley Online Library for rules of use; OA articles are governed by the applicable Creative Commons License

Oasis MCX 96-well μElution Plates (Waters Corporation, Milford, MA, USA), the samples were desalted in a semi-automated way using a Resolvex apparatus (Tecan, Männedorf, Switzerland) for automated desalting. The desalted preparations were aliquoted in subsamples in cases of sufficient peptide material.

To check for quality of the desalted preparations, a chromatographic separation on a monolithic reversed-phase column was performed. Small aliquots (10% of sample) were used for global proteome assessment. For the phospho-proteomes, aliquoted samples were enriched by Fe(III)-based immobilized metal-affinity chromatography (IMAC); this step was also performed in a semi-automated using an AssayMAP Bravo Platform (Agilent Technologies, Santa Clara, CA, USA), as described elsewhere.[32]

2.9 | Mass spectrometry (MS) and spectral search

For proteome and phosphoproteome analysis, peptides and phosphopeptides (IMAC enriched) were subjected to LC MS/MS measurements, according to described procedures.[33] In brief, analysis was performed by reversed-phase nano-LC MS/MS, using an Orbitrap Fusion Lumos mass spectrometer, as detailed elsewhere.[33] For peptide separation, the solvent gradient had an increasing organic content from 3% to 35%. The aqueous phase consisted of water and 0.1% formic acid; the organic phase consisted of acetonitrile and 0.1% formic acid. Ion generation was by electrospray ionization. Two independent analyses were performed with 23 (donors 1–3) and 10 (donor 3) platelet samples.

Label-free analysis of phosphopeptides was conducted as described.[15] Generated raw mass spectrometric data were searched against the human UniProt database, using Proteome Discoverer version 2.0 and Mascot as search engine. Identified peptides were filtered for high confidence corresponding to an FDR <1% at PSM level and a search engine rank of 1. Using precursor ion quantifier nodes, quantification was performed at the MS1 level. Only high-confidence annotated peptide sequences were collected, assignable to unique proteins in UniProt, with known phosphorylation, carbamidomethylation, and oxidation modifications. Per sample set, integrated mass peaks were summed to obtain normalized abundant values (NAVs).

2.10 | Sample availability and validation for label-free global proteome and phospho-proteome analysis

For the first dataset of label-free global proteomes, 30 platelet samples were analyzed from 3 healthy control donors (Table S1). Phospho-proteomes were obtained for 23 of the platelet samples, due to partly insufficient amounts of material during the sample preparation procedure (see Table S1).

For validation and completion purposes, residual protein amounts of all 10 platelet samples from donor 3 allowed a second, independent analysis (trypsinization, IMAC, LS-MS/MS analysis, engine database search) of both the global proteome and phosphoproteome (Table S1). This repetitive, validating analysis gave dataset 2 and allowed checking for the sample processing and inter-run variation of label-free mass-spectrometric data.[31,34]

2.11 | Data processing using Perseus and pathway analysis software

Per phosphopeptide analysis set, raw NAV intensities were uploaded into the Perseus software package from MaxQuant software. This package provides proteomic data processing and normalization options for the downstream analysis of quantitative proteomics results.[35] First, for each phosphopeptide with specific phosphosite, Pearson correlation coefficients were calculated between similar biological replicates. By applying a stringent filter, only those phosphopeptides were selected that were present in at least 2 out of 3 biological replicates per condition. After extraction of the filtered NAV data, log2-transformed changes per donor were calculated, relative to the corresponding unstimulated control sample. Subsequently, results from biological replicates were averaged, and a second filter was applied, in which per platelet condition those phosphopeptides were kept with a median log2 fold-change $>|\pm 1|$. These re-filtered data were used for functional enrichment analysis.

Selected proteins corresponding to the re-filtered phosphopeptides were applied to a functional enrichment analyzed in String.[36] Subsequently, Reactome (version 79) and KEGG (visited May 2022) pathways were retrieved from the functional enrichments, and sorted for lowest FDRs. Furthermore, enrichments of protein kinase-substrate interactions were looked up in the KSEA-APP, using as data source PhosphoSitePlus.[37–39] Cut-offs used were $p < .05$ and a substrate count of 1.

PhosphoSitePlus was also used for given phosphopeptides to predict their function as substrates for an atlas of 303 serine/threonine kinases.[40] The kinase entries were converted to common gene names. Log2 scores were recorded per phosphosite for all kinases, and positive scores were used for consistent kinase prediction. Protein and mRNA expression levels in human platelets were obtained from earlier analysis.[41]

15306860, 2024, 4, Downloaded from https://faseb.onlinelibrary.wiley.com/doi/10.1096/fj.202300360RR by Test, Wiley Online Library on [12/02/2024]. See the Terms and Conditions (https://onlinelibrary.wiley.com/terms-and-conditions) on Wiley Online Library for rules of use; OA articles are governed by the applicable Creative Commons License

2.12 | Quantitative label-free phosphoproteome validation analysis

Validation of the three-donor dataset was performed for 213 filtered phosphosites obtained via Reactome pathway analysis and for via 63 phosphosites of kinase-substrate links. Per phosphopeptide and phosphosite, ratios were calculated from raw NAVs of all interventions versus control condition ($n = 2–3$), averaged across donors, and log2-transformed and averaged across donors. Subsequently, the obtained values per phosphosite and per intervention condition were compared with the corresponding calculated ratios (log2 transformed), obtained in the replication dataset 2 for donor 3. In cases where the datasets contained two or more phosphopeptides per phosphosite, the log2-transformed ratios were averaged, in order to obtain one value per protein phosphosite.

2.13 | Tandem mass tag (TMT) platelet phosphoproteome analysis

Washed platelets (5.0×10^8/mL) from two additional healthy donors were exposed for 30 min to HUVEC, recollected, and then stimulated in the presence of 1 mM $CaCl_2$ with vehicle, CRP-XL (10 μg/mL) or α-thrombin (4 nM) for 3 min and 30 s, respectively. After stopping reactions with SDS and PhosSTOP (see above), lysed samples were subjected to quality checks, cysteine reduction, free sulfhydryl alkylation, and trypsin digestion with TMT 10-plex labels.[15] Pooled TMT-digested samples were subjected to an IMAC enrichment protocol, eluted, desalted, and subjected to single-shot LC–MS analysis, basically as described before.[15]

Raw data were searched against the human UniProt database, using Proteome Discoverer version 2.0, and further processed as described above. Lookup searches were confined to phosphopeptides with presumed differential up- or down-regulation by HUVEC or agonists. Data are expressed as log2-fold differences between individual samples from TMT pools (Datafile S1H).

2.14 | Statistics and bioinformatics

Data are given as means ± *SD*, unless indicated otherwise. Statistical significance was calculated in GraphPad Prism V.7 or higher or Excel Analyss32.xll software. For comparison of group data, a two-way or two-way ANOVA was used, as appropriate. Statistical significance was set at $p < .05$. Heatmaps were created with Perseus software. False discovery rates (FDR) for biological pathways were obtained from Reactome. Z-scores for kinase-substrate interactions were extracted from the KSEA database.

3 | RESULTS

3.1 | Suppressed collagen- and TF-dependent platelet activation of flowed blood exposed to endothelial cells

For establishing the effects of endothelial cells on collagen- and thrombin-dependent platelet responses in flowed whole blood, we modified an earlier method based on a sub-confluent HUVEC monolayer grown on collagen and TF using 200 μm deep Ibidi μ-luer slides. In the previous study, using a two-step protocol at low shear perfusion at room temperature, we determined potent antiplatelet and anticoagulant roles at 50% coverage of endothelial cells, suppressing the thrombus-forming activities of collagen and TF in the non-endothelial covered areas.[12] HUVEC were chosen as a consistent, low-passage endothelial cell type. Previous microfluidic tests furthermore confirmed that the collagen and TF surface induced platelet activation via GPVI and PAR1/4 receptors.[24]

For the present study, we coated glass coverslips with collagen alone or with collagen plus TF, and then cultured these with HUVEC (passage 4–6) until 50%–60% of area coverage. Control coverslips were treated similarly, but no HUVEC were present. Staining of the sub-confluently grown cells on coverslips demonstrated intact nuclei and a normal actin cytoskeleton, with (granular) VWF present in the peri-nuclear regions (Figure S1). For whole-blood perfusion experiments at high wall-shear rate of 1000 s^{-1}, we mounted the (endothelial cell-containing) coverslips in 50-μm deep, transparent microfluidic chambers.[42] The perfusions were carried out in a temperature-controlled environment of 37°C.

During whole-blood perfusion, we used multi-modular line-scanning microscopic imaging to monitor platelet and coagulation activation processes. In order to discriminate between GPVI- and PAR1/4-dependent effects on platelets, we employed two different protocols. In the first, coagulation was blocked by perfusing blood samples that were recalcified in the presence of PPACK over collagen. Alternatively, coagulation was controlled using collagen + TF-coated surfaces and perfusion of blood that was continuously recalcified using a two-pump system.[27]

In the high-shear flow runs not containing HUVEC, with either protocol, 3-min of blood flow resulted in the formation large thrombi of aggregated platelets (Figure 1A). In the coagulation protocol with TF, this was accompanied by massive fibrin fiber formation, starting at around 3 min (Figure 1B). Strikingly, the

15306860, 2024, 4, Downloaded from https://faseb.onlinelibrary.wiley.com/doi/10.1096/fj.202300360RR by Test, Wiley Online Library on [12/02/2024]. See the Terms and Conditions (https://onlinelibrary.wiley.com/terms-and-conditions) on Wiley Online Library for rules of use; OA articles are governed by the applicable Creative Commons License

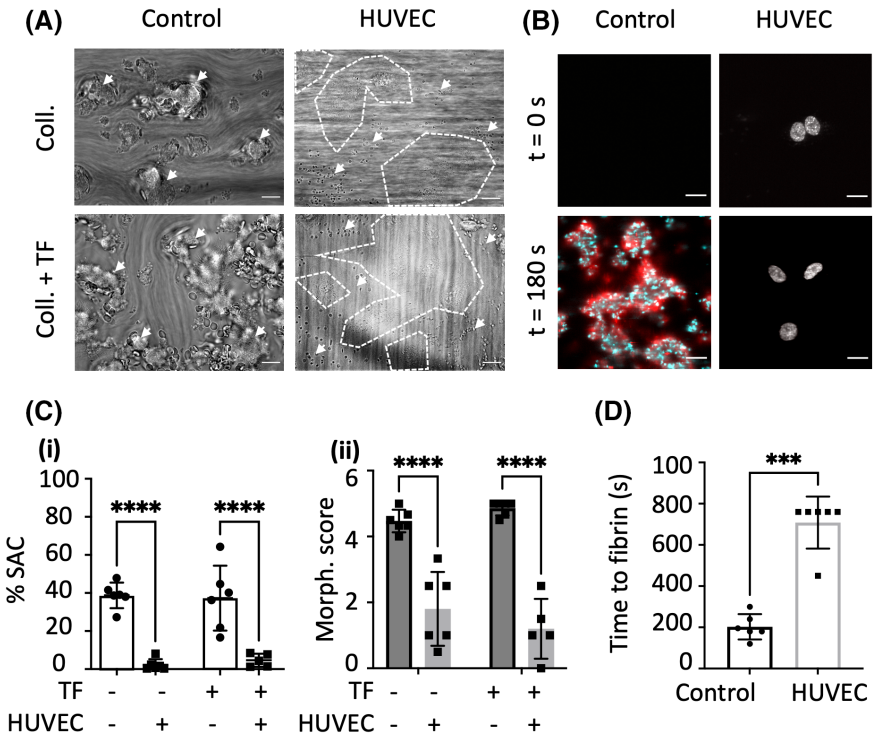

FIGURE 1 Sub-confluent endothelial cells abrogate platelet deposition and thrombus-fibrin formation in flowed whole blood. Sterile coverslips coated with collagen alone or collagen + TF were used as such (control) or were grown with HUVEC until 50%–60% coverage (37°C). After nuclear staining of the cells with Hoechst 33342, coverslips were inserted into a microfluidic chamber and perfused with whole blood containing autologous Fluo-4-loaded platelets (37°C). Blood samples were recalcified in the presence of PPACK before use (collagen condition). Alternatively, samples were continuously recalcified during flow without PPACK (collagen + TF condition). During flow, AF647-fibrinogen was present to track fibrin formation. Due to limited blood amounts, flow runs were stopped at 720 s, even when no fibrin was formed (in the presence of HUVEC). (A) Representative brightfield microscopic images after 180 s of blood perfusion. Shown are thrombi formed under control conditions, and single adhered platelets (white arrows) in the presence of HUVEC. Dotted lines indicate contours of patches of the endothelial cells. (B) Representative confocal fluorescence images of HUVEC nuclei (Hoechst, gray), platelets in thrombi (Fluo-4, cyan), and fibrin (AF647-fibrin, red) after 0 and 180 s of blood flow. (C) Quantification of platelet surface area coverage (i) and morphological thrombus score (ii) after blood flow. (D) Prolonged time to fibrin formation in the presence of HUVEC, obtained from confocal fluorescence images. Scale bars = 20 μm. Mean ± *SD* ($n = 5$–6); $^{**}p < .01$, $^{***}p < .001$ using a two-way ANOVA (panel C) or a Student *t*-test (panel D).

presence of 50%–60% covered HUVEC completely abrogated the thrombus and fibrin formation, even on areas where endothelial cells were absent (Figure 1A, B). Image quantification demonstrated a major, significantly reduced deposition of platelets with or without coagulation (Figure 1C,i). In addition, the formation of platelet aggregates was reduced when endothelial cells were present (Figure 1C,ii). With surfaces of collagen + TF, the presence of HUVEC greatly prolonged the time to fibrin formation (Figure 1D).

To monitor the endothelial effects on platelet activation under flow, we supplemented blood samples with autologous Fluo-4-loaded platelets and measured the rises in cytosolic $[Ca^{2+}]_i$ in videos captured at 5 Hz (Figure S2). On collagen alone (no coagulation), the majority of adhered platelets displayed a rapid increase in Fluo-4 fluorescence, as expected,[26] during the accumulation into a thrombus (Figure S2A). On collagen + TF (with coagulation), increases in platelet Fluo-4 fluorescence were substantially higher (Figure S2C). However, in both conditions, the partial coverage with HUVEC greatly suppressed the adhesion of platelets, which now were in majority low in Fluo-4 fluorescence (Figure S2B,D).

Quantification of the collagen-induced platelet $[Ca^{2+}]_i$ rises over time indicated a substantially higher integrated Fluo-4 signal above basal in the control condition, when compared to the HUVEC condition (Figure 2A,B). Comparing the areas under the curve, it appeared that the raised Fluo-4 fluorescence levels mostly disappeared, when HUVEC were present (Figure 2B,C). For the collagen + TF surface, even higher $[Ca^{2+}]_i$ rises over time were measured (Figure 2D,E). Also, the boosted Ca^{2+} response was suppressed in the HUVEC condition, where again raised Fluo-4 fluorescence levels disappeared (Figure 2F). Collectively, these results pointed to a potent, local

15306860, 2024, 4, Downloaded from https://faseb.onlinelibrary.wiley.com/doi/10.1096/fj.202300360RR by Test, Wiley Online Library on [12/02/2024]. See the Terms and Conditions (https://onlinelibrary.wiley.com/terms-and-conditions) on Wiley Online Library for rules of use; OA articles are governed by the applicable Creative Commons License

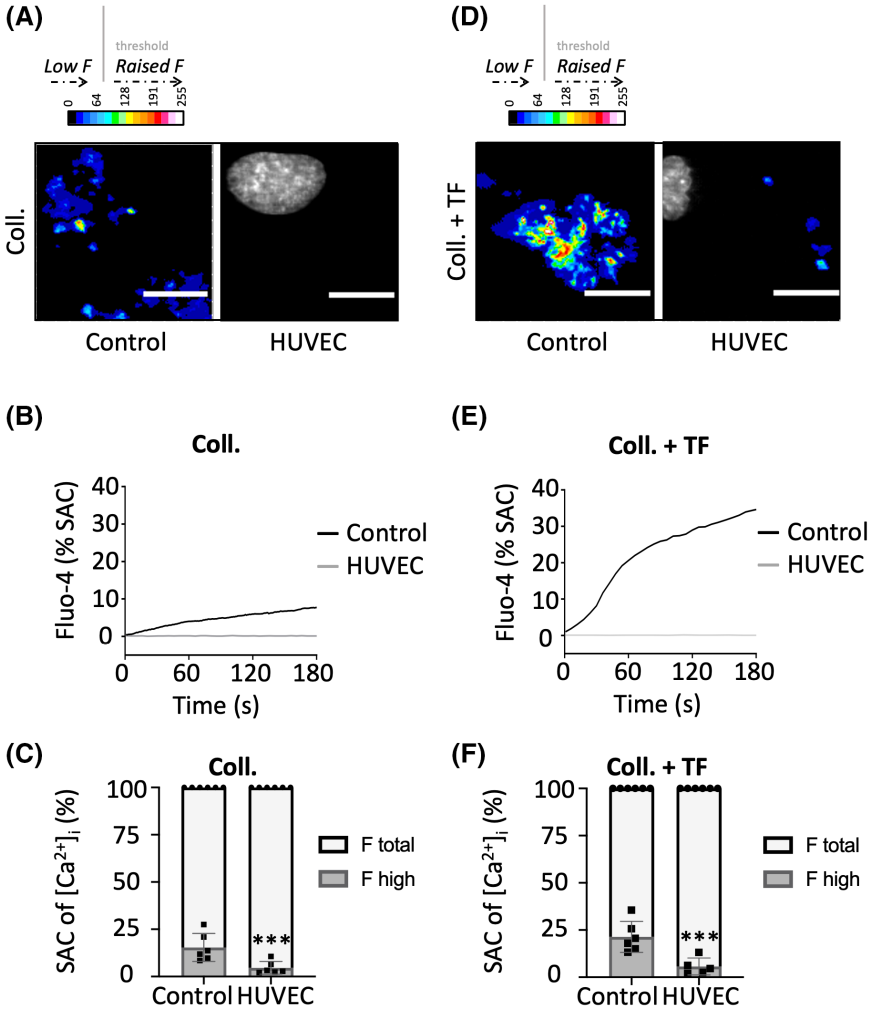

FIGURE 2 Sub-confluent endothelial cells suppress platelet $[Ca^{2+}]_i$ and rise in flowed whole blood. Blood samples, reconstituted with autologous Fluo-4-loaded platelets, were perfused through a microfluidic chamber coated with collagen alone (blocked coagulation) (A–C) or collagen + TF (allowed coagulation) (D–F), as for Figure 1. Time-lapse images of fluorescence were captured in real-time by confocal line-scanning microscopy during 180 s. (A, D) High-resolution end-stage fluorescence of Fluo-4-loaded platelets on collagen (A) or collagen + TF (D) in the absence (control) or presence of HUVEC. Rainbow colors indicate increased fluorescence, representing raised $[Ca^{2+}]_i$. (B, E) Cumulative Fluo-4 fluorescence over time of platelets on collagen (B) or collagen + TF (E) in the absence (control) or presence of HUVEC. Shown are representative traces. (C, F) Adhesion of platelets (SAC%) with low (basal $[Ca^{2+}]_i$, gray) or high (elevated $[Ca^{2+}]_i$, dark gray) fluorescence after 180 s. Mean ± *SD* ($n = 5–6$), $^*p < .05$, $^{**}p < .01$, $^{***}p < .001$, two-way ANOVA.

suppressing effect of endothelial cells on platelet signaling under flow under conditions of either blocked or permitted coagulation.

Interestingly, pretreatment of the HUVEC on collagen + TF coverslips with aspirin, the ecto-ATPase inhibitor ARL 67156 and/or the nitric oxide release inhibitor L-NNA did not improve the interaction or activation of Fluo-4-labeled platelets (Figure S3). Similarly, pretreatment of the cells with heparinase III, to remove heparan sulfates,[12] did not lead to increased platelet adhesion. This suggested that other factors than the expected endothelial-derived mediators (prostacyclin, nitric oxide, proteoglycans) contributed to the platelet-inhibiting effect.

3.2 | Suppressed GPVI- and PAR-induced platelet activation by endothelial cells under stasis

As a second approach to unravel endothelial effects on collagen- and thrombin-induced platelet activation, we performed experiments, where we incubated washed platelets with a HUVEC monolayer under static conditions and determined the effect of this on agonist-induced Ca^{2+} responses. For this purpose, we loaded platelets with the probe Calcium-6, which allowed to acutely monitor rises in $[Ca^{2+}]_i$ without an extra centrifugation step.[23] The dye-loaded platelets were incubated with HUVEC-containing or control wells (12-well plate, 30 min at 37°C),

15306860, 2024, 4, Downloaded from https://faseb.onlinelibrary.wiley.com/doi/10.1096/fj.202300360RR by Test, Wiley Online Library on [12/02/2024]. See the Terms and Conditions (https://onlinelibrary.wiley.com/terms-and-conditions) on Wiley Online Library for rules of use; OA articles are governed by the applicable Creative Commons License

after which samples were transferred to a 96-well plate, and automatically stimulated with agonist, i.e., CRP-XL (10 μg/mL, GPVI agonist) or thrombin (4 nM, PAR1/4 agonist), in the presence of 1 mM $CaCl_2$.

Measurement of the platelet count in subsamples before and after incubation with HUVEC showed a consistently high platelet recovery (Figure S4A), so that all wells contained the same numbers of platelets. Measurement of the $[Ca^{2+}]_i$ rises indicated for CRP-XL a slow-onset biphasic Ca^{2+} response (first peaking at about 3 min) and for thrombin a rapid high Ca^{2+} transient (peaking around 30 s), followed by a low secondary signal (Figure 3A,B), similarly as reported before in this well-plate setup.[23] With either agonist, the secondary Ca^{2+} response sustained over 30 min (1800 s). Prior exposure of Calcium-6-loaded platelets to HUVEC was of limited effect on the early $[Ca^{2+}]_i$ rise (3 min), but essentially abolished the long-term $[Ca^{2+}]_i$ rise (30 min), when quantified as fluorescence units or area under the curve (Figure 3A,ii–iii). Furthermore, the platelet exposure to HUVEC significantly diminished both the early (30 s) and the longer-term thrombin-induced $[Ca^{2+}]_i$ rise (30 min) (Figure 3B,ii–iii). A control experiment to assess the kinetics of inhibition indicated that a 1–5 min exposure to HUVEC was already sufficient to diminish the Ca^{2+} responses (Figure S4B). Collectively, these data pointed to a rapid onset and a long-term suppressing effect of agonist-induced platelet $[Ca^{2+}]_i$ rises following incubation with endothelial cells.

3.3 | Establishment of label-free phosphoproteomes of platelets exposed to endothelial cells

These effects on GPVI- and PAR-dependent $[Ca^{2+}]_i$ rises due to HUVEC exposure prompted us to investigate the platelet protein phosphorylation status. For this purpose, we determined the label-free phosphoproteome, as this procedure gives an unprecedented high number of phosphopeptides,[31,33] when compared to conventional multiplex analyses using stable isotopes.[15,17]

Reproducing the experimental conditions of the Ca^{2+} responses under stasis, we incubated washed platelets from 3 healthy donors in HUVEC-grown wells or in control wells (30 min, 37°C). After recollection, samples of the incubated platelets were treated with vehicle, CRP-XL (3 min or 30 min), or thrombin (30 s or 30 min) in the presence of 1 mM $CaCl_2$. This provided per donor 10 samples of

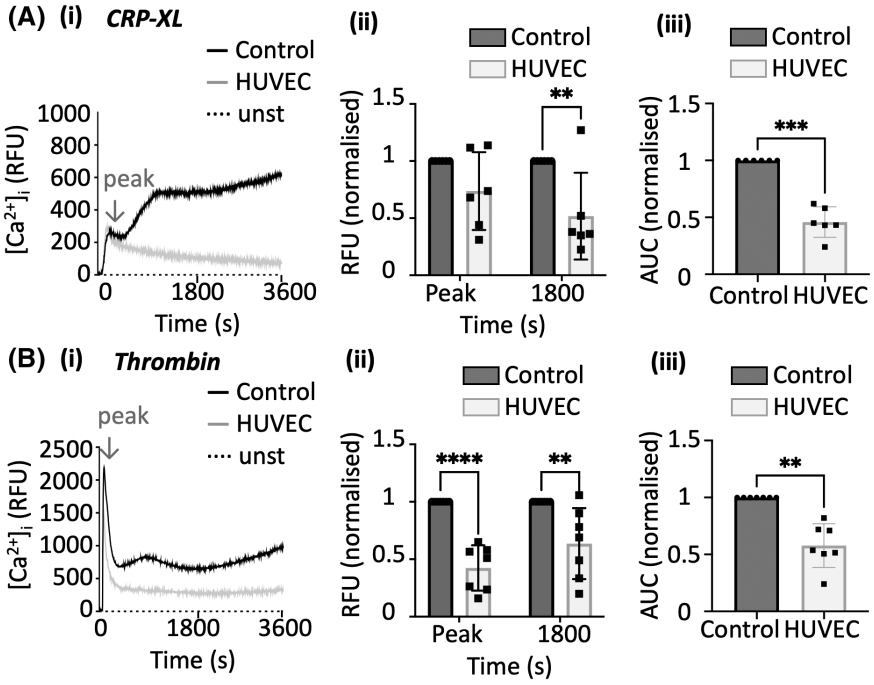

FIGURE 3 Platelet exposure to endothelial cells affects CRP-XL- and thrombin-induced $[Ca^{2+}]_i$ rises. Calcium-6-loaded platelets (3×10^8 in 1.5 mL) were incubated in 12-well plates containing confluent HUVEC or without HUVEC (control) for 30 min. The platelets were then carefully recollected, aliquoted over a 96-well plate, and automatically stimulated in the presence of 1 mM $CaCl_2$ with 10 μg/mL CRP-XL (A) or 4 nM thrombin (B). Injection speed of agonist addition was set to obtain optimal diffusion-limited exposure to platelets. (i) Shown are representative Calcium-6 fluorescence traces of platelets in the absence (control, black lines) or presence of HUVEC (gray lines). (ii) Furthermore, quantified $[Ca^{2+}]_i$ rises at agonist peak level (CRP-XL = 3 min, thrombin = 30 s) and after 30 min of either agonist. Relative fluorescence units (RFU) were normalized against control without HUVEC. (iii) Normalized areas on the $[Ca^{2+}]_i$ curves. Mean ± *SD* ($n = 5–6$), $^{**}p < .01$, $^{***}p < .001$, two-way ANOVA with Sidak's multiple comparison test (ii), or one sample *t*-test (iii).

15306860, 2024, 4, Downloaded from https://faseb.onlinelibrary.wiley.com/doi/10.1096/fj.202300360RR by Test, Wiley Online Library on [12/02/2024]. See the Terms and Conditions (https://onlinelibrary.wiley.com/terms-and-conditions) on Wiley Online Library for rules of use; OA articles are governed by the applicable Creative Commons License

HUVEC-exposed or control platelets, partly stimulated with CRP-XL or thrombin at early or late time points. Lysates of these platelet samples were used for the label-free global proteome and phosphoproteome analysis. In parallel, Ca^{2+} dye checks were performed to confirm the altered platelet responses to CRP-XL or thrombin (not shown).

For the quantitative label-free phospho-proteome analysis of platelet lysates, the workflow consisted of protein measurement, protein reduction, digestion at high throughput with trypsin, desalting, phosphopeptide enrichment using Fe(III) IMAC, and as a final analytical step LC MS/MS (Figure 4A). Qualitative checks were performed for a most reproducible quantitation. The 30 obtained global proteomes gave NAVs (normalized abundance values) of in total 3740 unique proteins, showing a high consistency between samples from the same donor ($R = 0.972 \pm 0.019$, mean $\pm$ *SD*) and also between samples across donors of the same condition ($R = 0.951 \pm 0.010$) (Table S2). This high similarity in global protein composition of the samples from (activated) platelets allowed subsequent comparison of the phosphoproteomes.

Due to limited platelet amounts and some sample loss during enrichment, phosphoproteomes were obtained from 23 samples, i.e., 9, 8, and 6 from donors 1, 2, and 3, respectively (Table S1). However, we kept 10 duplicate samples from donor 3, allowing a repeated analysis (see below). Mass spectrometry alignment and raw data normalization resulted in NAVs of 5463 assigned protein-linked (in UniProt) phosphopeptides, of which 77.50% were primarily allocated to a phospho-serine, 15.10% to a phospho-threonine and 7.40% to a phospho-tyrosine (Figure 4B). Annotation of the phosphopeptide sequences indicated that about 40% of the assignments referred to one or neighboring phosphosites (single, duplicate, or triplicate phosphorylations) (Datafile S1). Collectively, the phosphopeptides were derived from 1392 unique proteins. Calculation of Pearson's correlation coefficient across all phosphopeptide NAVs between samples indicated high reproducibility between biological replicates of the same condition (Figure 4C, black squares, mean $R = .86$). The constructed heatmap of *R* values also pointed to similarity between sample conditions with or without HUVEC exposure (Figure 4C, white squares). Overall, this pointed to consistent effects on the label-free phosphoproteome of platelet stimulation with CRP-XL or thrombin. In this respect, the condition CRP-XL/late deviated most strongly from the control condition (no HUVEC, no agonist).

The NAV ratio values per phosphopeptide versus the control condition were calculated, averaged across donors, and then ranked according to the changes seen with CRP-XL/late. The resulting log2-transformed ratios confirmed a certain pattern of changes in phosphopeptides by HUVEC exposure, larger changes by platelet stimulation with thrombin, and largest changes upon early/late stimulation with CRP-XL (Figure 4D).

3.4 | Biological pathway analysis of endothelial- and agonist-regulated protein phosphorylation changes

Given the massive dataset of 5463 phosphopeptides, in part redundant for specific protein phosphosites, we searched for ratioed peptide differences between samples with a likely physiological relevance. Therefore, we first determined per donor for all 5463 values the log2-transformed fold changes (log2 FC) versus unstimulated control samples. Using the analysis program Perseus, two stringent filters were applied to select changes of (i) phosphopeptides identified in ≥2 donors, and (ii) cut-offs with a log2 FC ≥ |±1|. This resulted in a total of 1472 phosphorylated proteins with an assumedly relevant regulation in any condition. The analysis was hence continued for the 8 conditions with $n \geq 2$ versus control.

The corresponding proteins were then checked in the KEGG (Genome.jp/kegg) and Reactome[43] pathway databases, after functional enrichment analyses in String. Submission of the selected 1472 phosphoproteins to KEGG gave 18 significantly enriched pathways for the HUVEC-exposed samples (Datafile S1A). Herein, the pathway 'Platelet activation' came out with lowest FDR of 2.51×10^{-9}. Several other platelet-related pathways were retrieved, namely 'Rap1 signaling pathway', 'Regulation of actin cytoskeleton' and 'cGMP-PKG signaling pathway' (Table S3). Altogether, 58 phosphorylated proteins were obtained by KEGG, among which 14 protein kinases and 8 plasma membrane receptors & channels, mostly appearing in multiple pathways.

To obtain better coverage of the regulated phosphoproteins, Reactome enrichment analysis was performed with the String package. This resulted in a list of 792 phosphoproteins, appearing in the 26 most significantly enriched biological pathways (median FDR across 8 conditions from 1.96×10^{-10} to 1.93×10^{-2}). Heatmapping the FDR values (log2 FC) illustrated a consistent regulation per pathway for the majority of experimental conditions (Figure S5A). Several of the most significantly regulated pathways were again linked to platelet activation ('Signaling by Rho GTPases', 'Hemostasis', 'Platelet activation', 'Signal transduction', 'Response to elevated platelet cytosolic Ca^{2+}', 'Platelet aggregation', 'Rho GTPase effectors', 'Integrin signaling', and 'Platelet degranulation).

For each Reactome pathway, the contribution of each of the 792 phosphoproteins was checked per experimental condition (exposure to HUVEC, CRP-XL, or thrombin early/late). This effort indicated a lower FDR for the HUVEC and the thrombin-early conditions than for the

15306860, 2024, 4, Downloaded from https://faseb.onlinelibrary.wiley.com/doi/10.1096/fj.202300360RR by Test, Wiley Online Library on [12/02/2024]. See the Terms and Conditions (https://onlinelibrary.wiley.com/terms-and-conditions) on Wiley Online Library for rules of use; OA articles are governed by the applicable Creative Commons License

CRP-XL conditions (Figure S5B). Unsupervised clustering analysis, separating all conditions, indicated that the ratioed changes present in platelets exposed to HUVEC did well separate from the non-HUVEC condition (Figure 5A). We thus obtained prominent clusters (color-coded in blue) of exclusively altered phosphorylations by HUVEC, CRP-XL, or thrombin (Figure 5B).

3.5 | Protein kinase-substrate analysis of endothelial- and agonist-regulated platelet protein phosphorylation changes

Considering that protein kinases can act by phosphorylation of other kinases, we also confined the 1472 regulated phosphorylated proteins to 144 protein kinases.

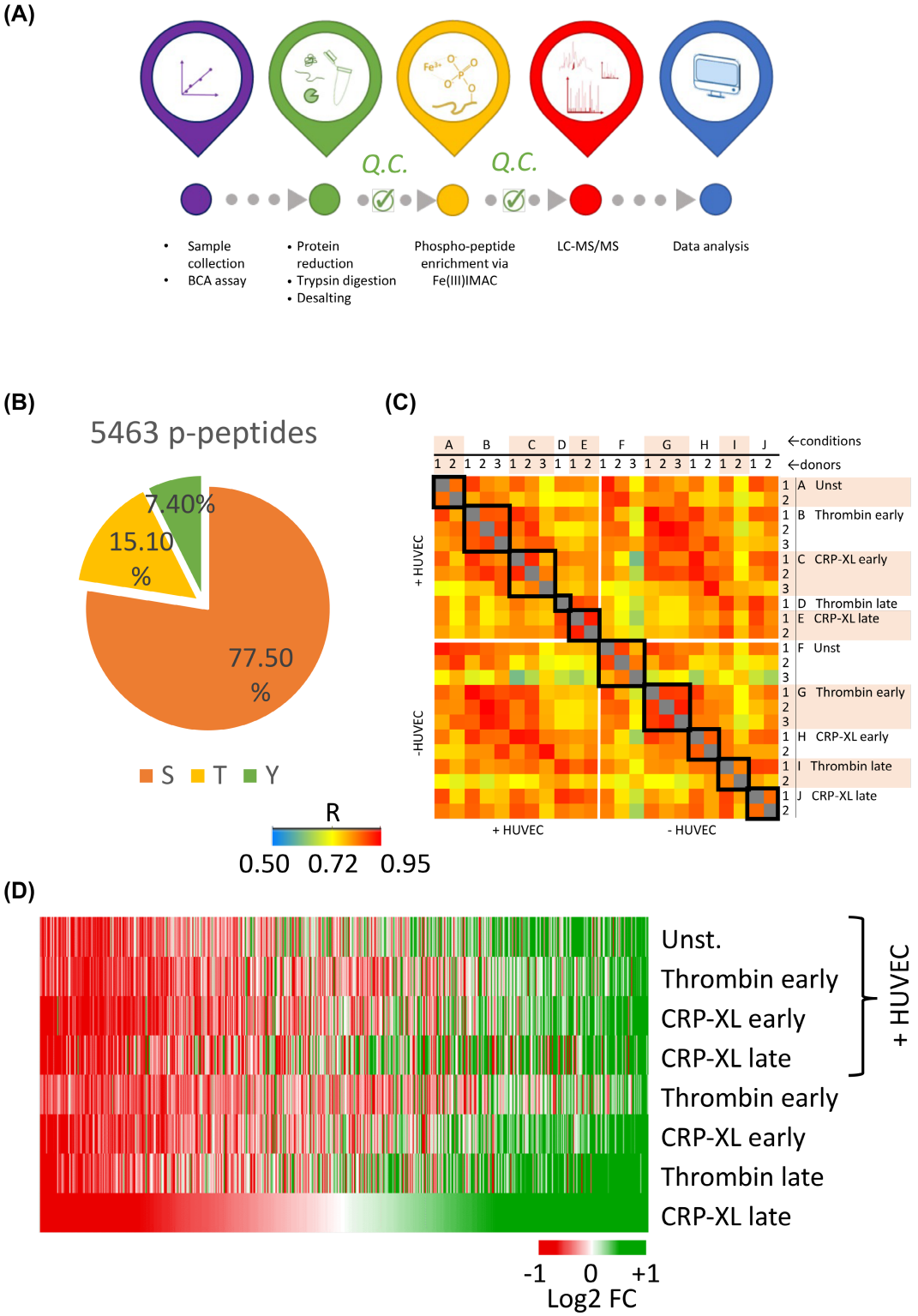

15306860, 2024, 4, Downloaded from https://faseb.onlinelibrary.wiley.com/doi/10.1096/fj.202300360RR by Test, Wiley Online Library on [12/02/2024]. See the Terms and Conditions (https://onlinelibrary.wiley.com/terms-and-conditions) on Wiley Online Library for rules of use; OA articles are governed by the applicable Creative Commons License

FIGURE 4 Sample processing for establishing high-throughput label-free phosphoproteomes of platelets exposed to endothelial cells. Platelets were incubated for 30 min in 12-well plates containing confluently grown HUVEC or control wells without. Samples were activated with CRP-XL or thrombin (early or late) for 3 healthy donors and 10 conditions. Samples analyzed per donor with variables are listed in Table S1. (A) Technical bottom-up workflow to obtain label-free global proteomes and phospho-proteomes. Total proteins of lysed platelet samples were determined with a BCA assay; samples were digested with trypsin. Subsamples were taken for analysis of the global proteome; samples were subjected to phosphopeptide enrichment by single-step Fe(III)-based IMAC. (B) Mass-spectroscopy performed via LC–MS/MS, and spectral data alignment resulted in 5463 identified phosphopeptides (77.50% Ser, 15.10% Thr, 7.40% Tyr). (C) Heatmap of Pearson's intensity correlation R of all samples per condition, showing high consistency of NAVs per phosphosite between biological replicates (black squares). Note further overall pattern similarity of conditions with or without HUVEC (white squares). (D) Effect-size heatmap of log2-transformed fold changes (log2 FC) per phosphopeptide, obtained by ratioing versus the unstimulated control sample per donor. Phosphopeptides ($n = 5463$) were filtered for presence in ≥2 biological replicates per condition. Shown are medians of log2 FC, sorted according to the changed ratio with CRP-XL/late (no HUVEC). Color bar separates downregulated (red), unchanged/absent (white), or upregulated (green).

From these, 56 kinases were found to be phosphosite regulating, as sorted via median Z scores across all 8 conditions. The most significantly upregulated (positive Z scores, blue) and downregulated (negative Z scores, red) phosphosites are presented in the heatmap of Figure S6A. For each of the kinases, a substrate enrichment analysis was performed, searching for phosphopeptides in our database, using PhosphoSitePlus.[44] This resulted in a total of 143 regulated kinase substrates per condition (Figure S6B). Clustering analysis of these kinase substrates (Figure 6C) confirmed that different sets of phosphosites were linked to conditions of HUVEC, CRP-XL, or thrombin (Figure 6D). Together, the pathway and kinase substrate analysis revealed different phosphoproteome signatures by platelet exposure to HUVEC, CRP-XL, and/or thrombin.

3.6 | Consistency of differentially regulated phosphorylation signatures

Knowing the variability of conventional phosphoproteomics,[15] likely extending to label-free phosphoproteomes, we performed a de novo analysis using duplicate platelet preparations from donor 3 (labeled as D3', all 10 conditions). This involved a new trypsin treatment, IMAC enrichment, LS MS/MS, spectral alignment, and data search. The second analysis provided 6979 phosphopeptides matching to unique proteins for all conditions (Datafile S1F).

For the phosphoproteins obtained in the two procedures (Datafile S1G), we compared the mean log2-transformed values versus control condition (no HUVEC, no agonist). Reactome analysis revealed 192 common phosphosites in both datasets, which contained the majority of phosphoproteins in the 26 selected biological pathways (Figure S6A). Importantly, in both datasets, most phosphoproteins were commonly down-regulated or up-regulated, at amounts ranging from 71% to 85% per experimental condition (Figure S6B). The similarity increased even further to 89%–97%, using an arbitrary tolerance level of log2 FC of |±0.15| for non-regulated phosphosites. The constructed correlation heatmap of log2 FC for both datasets and all conditions indicated consistent changes in the platelets exposed to HUVEC, early/late CRP-XL, or thrombin (Figure S6B). Accordingly, our repeated analysis pointed to sufficient reliability and to limited inter-donor variation for the 192 obtained phosphoprotein changes.

We then examined the signs of specific protein phosphorylation changes (up- or downregulation) by exposure to HUVEC, CRP-XL, or thrombin (means of conditions) for dataset 1 (donors D1-3) and dataset 2 (donor D3'), confined to the 63 phosphosites linked to protein kinases (Table S4A) and 213 phosphosites from Reactome pathways (Table S4B). There appeared to be a subset 42 phosphorylation changes that were oppositely regulated by HUVEC exposure or by (single) agonist stimulation (Table S5). Interestingly, a larger subset of 110 phosphorylation changes were commonly up- or down-regulated by these interventions (Table S5). Combined analysis of datasets 1 and 2 resulted in a list of 44 proteins of phosphosites with opposite regulation by HUVEC or by CRP-XL/thrombin (Table 1, details in Table S6).

In order to validate these findings, a new phosphoproteome analysis was performed using platelets from two additional donors (D4 and D5). The isolated platelets were again exposed to HUVEC (30 min) and/or activated with CRP-XL (3 min) or thrombin (30 s). For this purpose, we choose for an independent method, i.e., conventional stable isotope (TMT, tandem mass tag) analysis, which provides mass spectrometry ratio values of phosphopeptide fragments for all compared samples. When extracting the results of the two TMT analyses, we could retrieve the majority of 44 regulated phosphopeptides (Datafile S1H). Inspection of the log2 FC across all 5 donors indicated

15306860, 2024, 4, Downloaded from https://faseb.onlinelibrary.wiley.com/doi/10.1096/fj.202300360RR by Test, Wiley Online Library on [12/02/2024]. See the Terms and Conditions (https://onlinelibrary.wiley.com/terms-and-conditions) on Wiley Online Library for rules of use; OA articles are governed by the applicable Creative Commons License

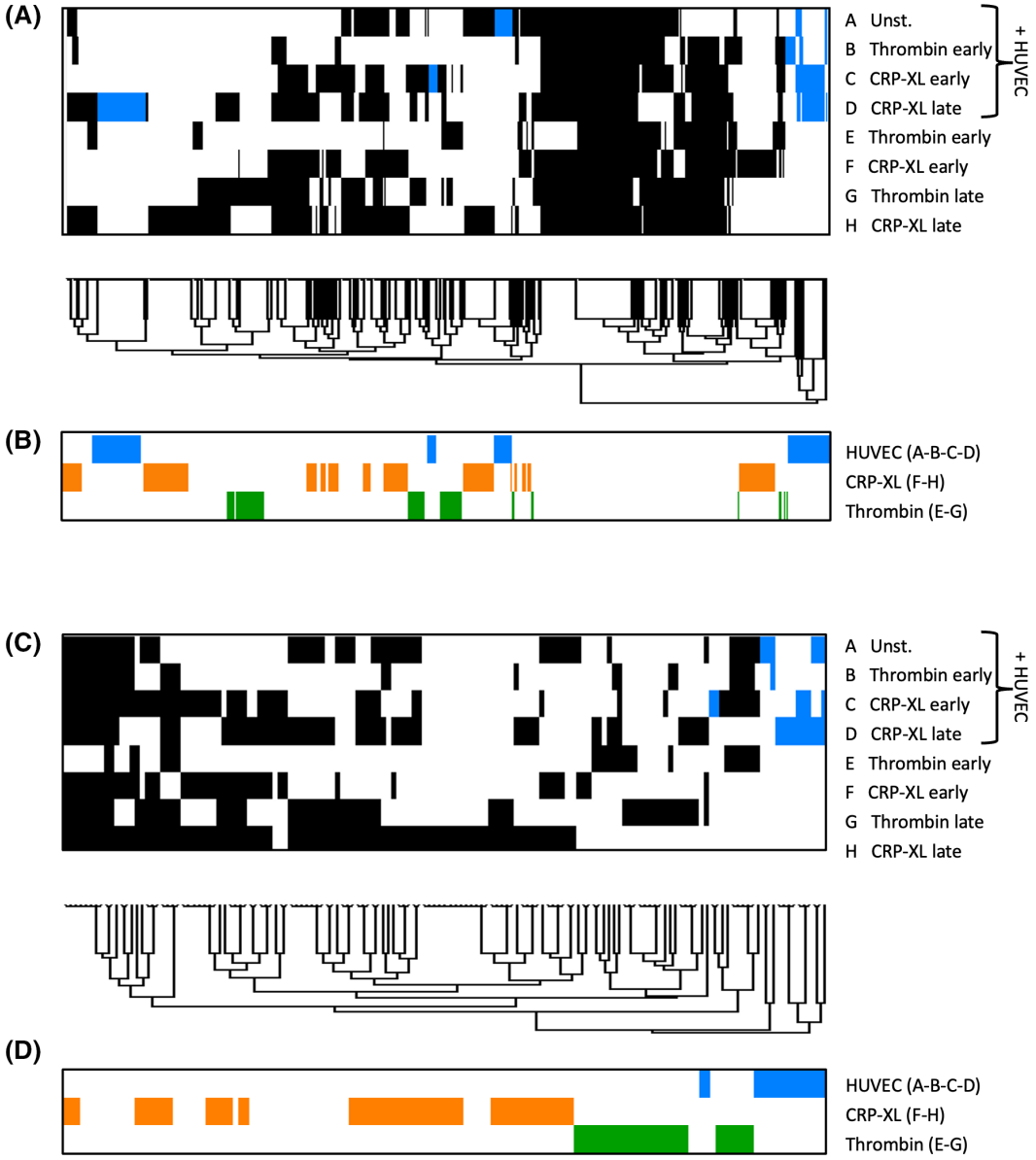

FIGURE 5 Reactome and protein kinase enrichments of endothelial- and agonist-regulated platelet phospho-proteomes. (A, B) Unsupervised clustering analysis of regulated phosphoproteins from 26 Reactome enriched pathways per experimental condition. Data derived from Figure S5. (A) Assignment matrix of pathway regulation (black = passed filters per condition; blue = idem for only regulation by HUVEC; white = unchanged or absent). (B) Separation of data set according to exclusive regulation by HUVEC (blue), CRP-XL (orange), or thrombin (green). (C, D) Unsupervised clustering analysis of phospho-substrates for kinases enriched in PhosphoSitePlus per experimental condition. Data derived from Figure S6. (C) Assignment matrix of phosphoprotein regulation (black = passed filters per condition; blue = idem for only regulation by HUVEC; white = unchanged or absent). (D) Separation of data set according to exclusive regulation by HUVEC (blue), CRP-XL (orange), or thrombin (green).

a high similarity for all datasets, with Pearson correlation coefficients >.6 for per experimental condition (HUVEC, CRP-XL, thrombin). The constructed heatmap—comparing all 44 phosphoproteins—showed a consistent opposing phosphorylation by platelet exposure to HUVEC or CRP-XL/thrombin (Figure 7). Taken together, this combined analysis led to a set of phosphorylation changes that was uniquely evoked by platelet exposure to HUVEC.

3.7 | Assessment of differentially regulated protein kinases in platelets exposed to HUVEC or agonists

Using an earlier protein function classification scheme,[41] we ordered many of the 44 opposite-regulated phosphoproteins to: 'Membrane channels & receptors', 'Protein kinases & phosphatases', 'Signaling & adapter proteins', and 'Small GTPases & regulators' (Table 1). The set included

15306860, 2024, 4, Downloaded from https://faseb.onlinelibrary.wiley.com/doi/10.1096/fj.202300360RR by Test, Wiley Online Library on [12/02/2024]. See the Terms and Conditions (https://onlinelibrary.wiley.com/terms-and-conditions) on Wiley Online Library for rules of use; OA articles are governed by the applicable Creative Commons License

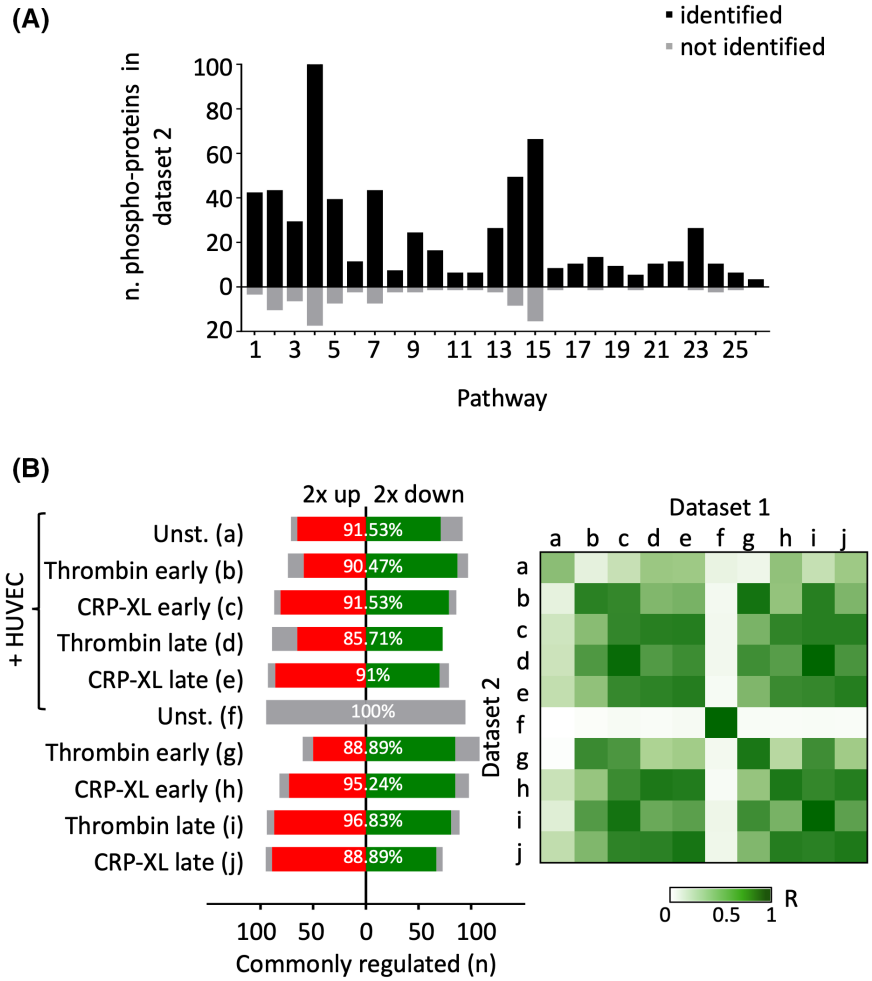

FIGURE 6 Confirmation of pathway-enriched changes in endothelial- and agonist-regulated platelet phosphoproteomes. Per phosphosite, averaged ratioed values (from raw NAVs) versus the control condition from three donors (dataset 1) were compared with similar rationed values from donor 3 (dataset 2), with as matrix the phosphopeptides obtained from the Reactome pathway enrichment. In total, 192 common phosphosites were retrieved from the two datasets (Datafile S1D–F). (A) Numbers of identified and not identified phosphoproteins in dataset 2 per Reactome pathway. For description of the pathways 1–25, see Figure 5. (B) (i) Numbers of phospho-proteins per experimental condition, which were commonly upregulated (red) or downregulated in datasets 1 and 2. Gray bars indicate assumed non-regulated phospho-proteins, i.e., log2 FC < |±0.15|. (ii) Heatmap of correlation coefficients (multiple R) between experimental conditions for all 192 common phospho-proteins, comparing dataset 1 and dataset 2. Note the similar coloring pattern in each quartile, pointing to overall high consistency of the phosphorylation changes in either dataset.

(co)receptors for thrombin (F2R, F2RL3), thromboxane (TBXA2R), collagen (FCER1G), integrins (ITGA2, ITGB3) and junctional proteins (F11R, TJP2, PECAM1). Also present were key regulating protein kinases downstream of GPVI (SRC, SYK, BTK), and isoforms of protein kinase C (PRKCQ) and protein kinase A (PRKAR1A); furthermore key signaling proteins of integrin activation (TLN1, RASA3).[17] While all these proteins contribute to the Ca^{2+} signal generation in platelets, it still needs to be established for instance by mutagenesis, which of the phosphorylation sites contribute to the endothelial suppression of platelet Ca^{2+} signaling. Of note, the list of Table 1 is obtained by two consecutive sets of phospho-proteome analysis, hence with independent validation.

For the 42 phosphorylated peptides on serine/threonine residues, we used the PhosphoSitePlus atlas to predict their suitability as substrates for 303 common protein kinases.[40] Summing the positive prediction scores per class of kinases indicated strong contributions of mitogen-activated protein kinases (MAPK), dual-specificity tyrosine-regulated kinases (DYRK), cyclin-dependent kinases (CDK), serine/threonine kinases (STK), and protein kinases C (PKC) (Figure 8). Proteins and transcripts from members of these classes are highly expressed in human platelets. A lower positive substrate prediction was obtained for Toa serine/threonine kinases (TOAK), Nek serine/threonine kinases (NEK), G protein-coupled receptor kinases (GRK), and homeodomain-interacting kinases

15306860, 2024, 4, Downloaded from https://faseb.onlinelibrary.wiley.com/doi/10.1096/fj.202300360RR by Test, Wiley Online Library on [12/02/2024]. See the Terms and Conditions (https://onlinelibrary.wiley.com/terms-and-conditions) on Wiley Online Library for rules of use; OA articles are governed by the applicable Creative Commons License

TABLE 1 Identified phosphosites with opposite regulation by HUVEC or thrombin/CRP-XL stimulation.

C10—Membrane receptors & channels (n = 15)
ADAM10 (T719), ADAM17 (T735), F11R (S287), F2R (S418, Y420), F2RL3 (S381, S382), FCER1G (Y65, S69), ITGA2 (T1177), ITGB3 (T781, Y785), PECAM1 (Y713), SCARF1 (S753), SLC9A1 (S785), STOM (S18), TBXA2R (S331), TBXA2R (T337), TJP2 (S986)
C15—Protein kinases & phosphatases (n = 13)
BTK (T184), GRK5 (S484), LATS1 (T246), MARK2 (T596), PAK2 (Y139, S141), PRKCQ (T538, Y545), PRKAR1A (S83), PTPRJ (S1009), SRC (S17), STK3 (T336), STK4 (T340), SYK (S295, Y296), WNK1 (S2032)
C18—Signaling & adapter proteins (n = 6)
ARAP1 (S729), DBNL (S274), DAPP1 (S276), DOK1 (Y449), NCK1 (S85), TLN1 (S446)
C19—Small GTPases & regulators (n = 8)
ARHGAP18 (T158), ARHGAP25 (S362), ARHGEF12 (T736), DOCK2 (S1706), FGD3 (S547), RAP1GAP2 (S507), RASA3 (Y807, S809), RGL2 (S761)
C21—Miscellaneous (n = 2)
LMNA (S22), KIF2A (T97)

Note: Proteins ($n = 44$) are ordered according to function class. Note the presence of only tyrosine phosphorylation sites in PECAM1 and DOK1. Underlined phosphosites were previously reported as regulated by (ant) agonists.[17] For full data, see Table S6.

(HIPK). Proteins and mRNAs of the latter kinase classes have also relatively low expression levels in platelets. Interestingly, only few of the phosphosites scored positively as substrates for PKA and PKG (Figure 8). Taken together, these data point endothelial cell-evoked activation of a multi-kinase network in platelets, extending regulation by PKA and PKG.

4 | DISCUSSION

In this paper, we first describe an improved vessel-on-a-chip microfluidic model, which allowed single-step whole blood perfusion over a collagen and TF with partly confluent endothelial cells (50%–60%) at high-shear rate and physiological temperature of 37°C. The use of a shallow flow chamber in combination with brightfield and confocal microscopy allowed monitoring in real time of platelet adhesion and activation in the presence of endothelial cells. On collagen/TF-coated surfaces, we observed that partial coverage of HUVEC was sufficient to block platelet activation and fibrin formation. As cell source, we choose for HUVEC as a robust, low-passage endothelial cell type, which is standardly available in the laboratory setting. Confocal monitoring of Fluo-4-loaded platelets in whole-blood samples also indicated that the presence of endothelial cells abrogated the rises in $[Ca^{2+}]_i$ in platelets. Our data hence point to acute antiplatelet and anticoagulant activities of the HUVEC at physiological temperature, suggesting the presence of powerful mediators released by or present on these cells. In contrast, when using a similar flow assay with hepatocyte progenitor cells, high platelet deposition and fibrin formation has been observed.[45] In earlier flow studies, using collagen and TF surfaces, we established that platelet activation was evoked by the collagen receptor GPVI and the thrombin receptors PAR1/4.[24] When compared to an earlier two-phased flow studies carried out at room temperature,[12] the current data indicate that whole-blood flow at high shear and physiological temperature leads to an even stronger HUVEC-dependent suppression of platelet and coagulant activities.

To disclose how the endothelial cells altered platelet signaling pathways, we used a separate setup, in which washed platelets under stasis were exposed to HUVEC, and subsequently were stimulated with GPVI agonist CRP-XL or with PAR1/4 agonist thrombin. Measurements using Calcium-6 loaded platelets indicated an initial $[Ca^{2+}]_i$ peak with thrombin and a biphasic $[Ca^{2+}]_i$ rise with CRP-XL, as described before.[23] Also with this static assay, the exposure of platelets to endothelial cells led to a consistent downregulation of the agonist-induced Ca^{2+} signals, an effect that was detectable after several min and progressed up to 30 min.

The latter results prompted us to establish the effects of platelet exposure to HUVEC and/or CRP-XL or thrombin on the phosphoproteome, using platelets from three donors (D1-3). To establish this, we used a novel label-free phospho-proteomic approach.[31] For reproducible sample processing, we performed desalting and phosphopeptide enrichment steps semi-automated in a well plate.[32,33] After sample workup and mass spectrometry, we obtained high-content label-free (phospho)proteomes of the platelets, whether or not exposed to HUVEC and activated with CRP-XL or thrombin at early (3 or 0.5 min) or late (30 min) time points. For 3 donors and 23 samples, after quality check, this resulted in the quantification as NAVs of 5463 phosphopeptides, which were ratioed versus the control condition, and expressed as log2 fold changes.

Given the multitude of partly overlapping phosphopeptides, we applied stringent filters to select relevant changes in phosphorylation, which effort reduced the set to 1472 phosphopeptides assigned to unique proteins. After setting cut-off values of log2 FC > |±1|, the Reactome database reported low FDRs for multiple hemostatic pathways, thus reducing the list to 792 phosphoproteins. Using the KSEA App, we obtained a list of 143 regulated phosphoprotein substrates linked to predicted protein kinases. Heatmapping and clustering indicated that 255 phosphorylations in platelets were altered by HUVEC exposure or by CRP-XL or thrombin stimulation. The overall

15306860, 2024, 4, Downloaded from https://faseb.onlinelibrary.wiley.com/doi/10.1096/fj.202300360RR by Test, Wiley Online Library on [12/02/2024]. See the Terms and Conditions (https://onlinelibrary.wiley.com/terms-and-conditions) on Wiley Online Library for rules of use; OA articles are governed by the applicable Creative Commons License

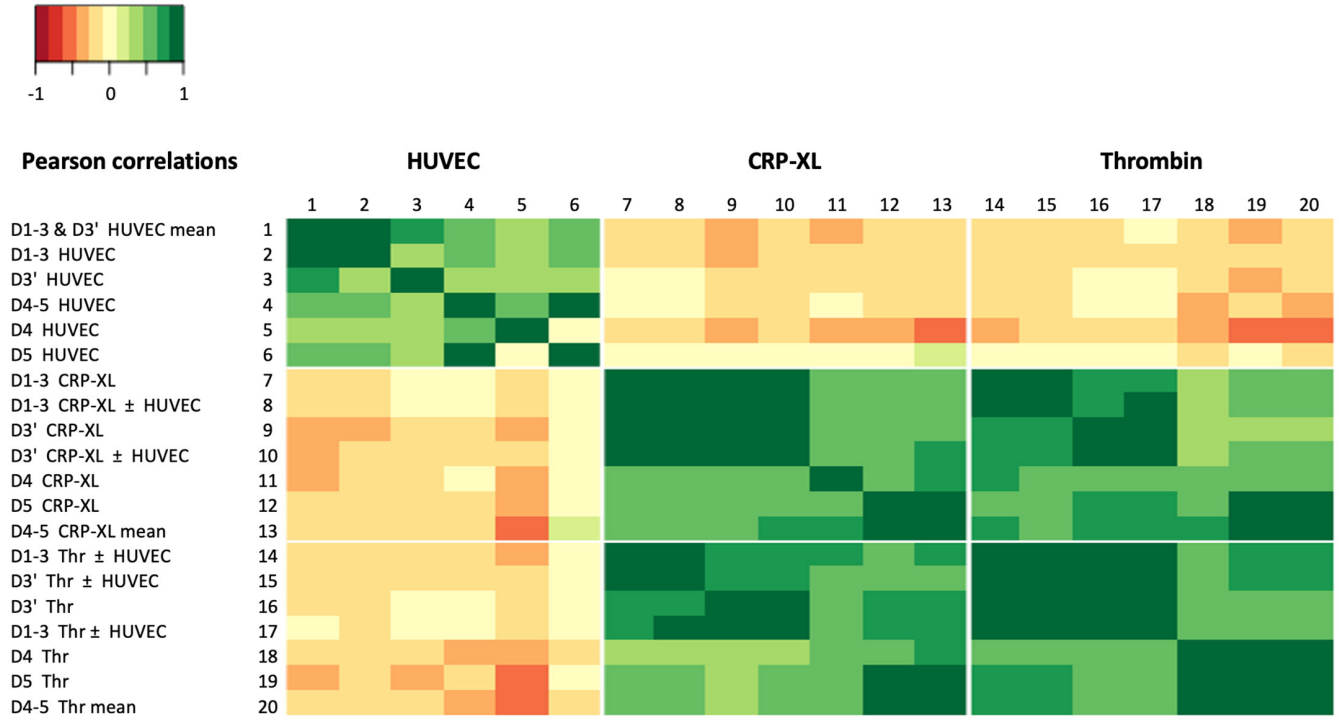

FIGURE 7 Validation and consistency of differentially regulated phosphoproteins in platelets exposed to endothelial cells or agonists. Washed platelets (5.0×10^8/mL) from donors 4 and 5 exposed to vehicle medium or HUVEC (30 min) and stimulated with CRP-XL (10 μg/mL, 3 min) or thrombin (4 nM, 30 s), as indicated. Proteins in lysed samples were trypsin digested with TMT 10-plex labels, pooled per donor, and enriched phosphopeptides were separated by mass spectrometry. Quantitatively analyzed were 42 phosphopeptides with potential differential regulation (Table 1), and expressed as log2 fold changes. Shown is a Pearson correlation heatmap comparing changes per dataset (D1-3, D3', D4, D5) and experimental condition (HUVEC, CRP-XL, Thr). Note consistency between HUVEC conditions and opposite effects of HUVEC versus agonists. Raw datasets are in Datafile S1H,I.

changes in protein phosphorylation could be confirmed in a second, independent analysis of platelets from donor 3 (D3′, 10 conditions).

Phosphopeptide ratio analysis revealed an overall high correlation of the two datasets (D1-3 and D′) and showed a consistent set of phosphorylation changes induced by HUVEC exposure or by CRP-XL or thrombin stimulation. We found opposite effects for about 20% (44 phosphosites) of the phosphorylation changes. On the other hand, it appeared that 60% of the phosphorylation changes were commonly increased or decreased by platelet exposure to HUVEC or platelet stimulation. Validating experiments with platelets from two additional donors (D4-5) confirmed the set of 44 opposingly regulated phosphoproteins. Collectively, these findings suggest a resetting of the platelet phosphorylation profile, induced by the blood drawing and platelet isolation, which becomes reverted by exposure to physiologically relevant inhibitory or stimulatory conditions. However, this suggestion needs to be proven.

Our results significantly extend those from studies in the literature, where the platelet phosphoproteome was mostly assessed in response a single agonist or inhibitor.[46] An earlier report indicated partly common phosphorylation changes in platelets induced by the agonist ADP and the prostacyclin analog iloprost.[17] Strikingly, comparison of the present changes induced by platelet exposure to HUVEC reveals no more than partial similarity with previous (stable isotope) phosphoproteome changes in response to prostacyclin analog[16,17] or a nitric oxide generation[18] (Table 1). The lack of effect of HUVEC treatment with aspirin and L-NNA in the microfluidic assay also suggested that these endothelial-derived mediators are not the only or most essential factors that regulate the phosphorylation changes in platelet proteins.

Comparing for all donors (D1-5) the 44 opposingly regulated phosphoproteins by HUVEC or agonists showed high consistency in both the sign and size of the changes. Closer examination of the 42 serine/threonine phosphosites using the PhosphoSitePlus atlas revealed strongest contributions of the classes of mitogen-activated protein kinases (MAPK), dual-specificity tyrosine-regulated kinases (DYRK), cyclin-dependent kinases (CDK), serine/threonine kinases (STK), and protein kinases C (PKC). The literature provides no more than limited information on how these protein kinase classes in platelets are affected by bio-mediators. An exception being the proposed role of p38 (MAPK11-14) and PKCδ (PRKCD) in thromboxane-dependent responses.[47,48] On the other hand, the best-known kinases regulating

15306860, 2024, 4, Downloaded from https://faseb.onlinelibrary.wiley.com/doi/10.1096/fj.202300360RR by Test, Wiley Online Library on [12/02/2024]. See the Terms and Conditions (https://onlinelibrary.wiley.com/terms-and-conditions) on Wiley Online Library for rules of use; OA articles are governed by the applicable Creative Commons License

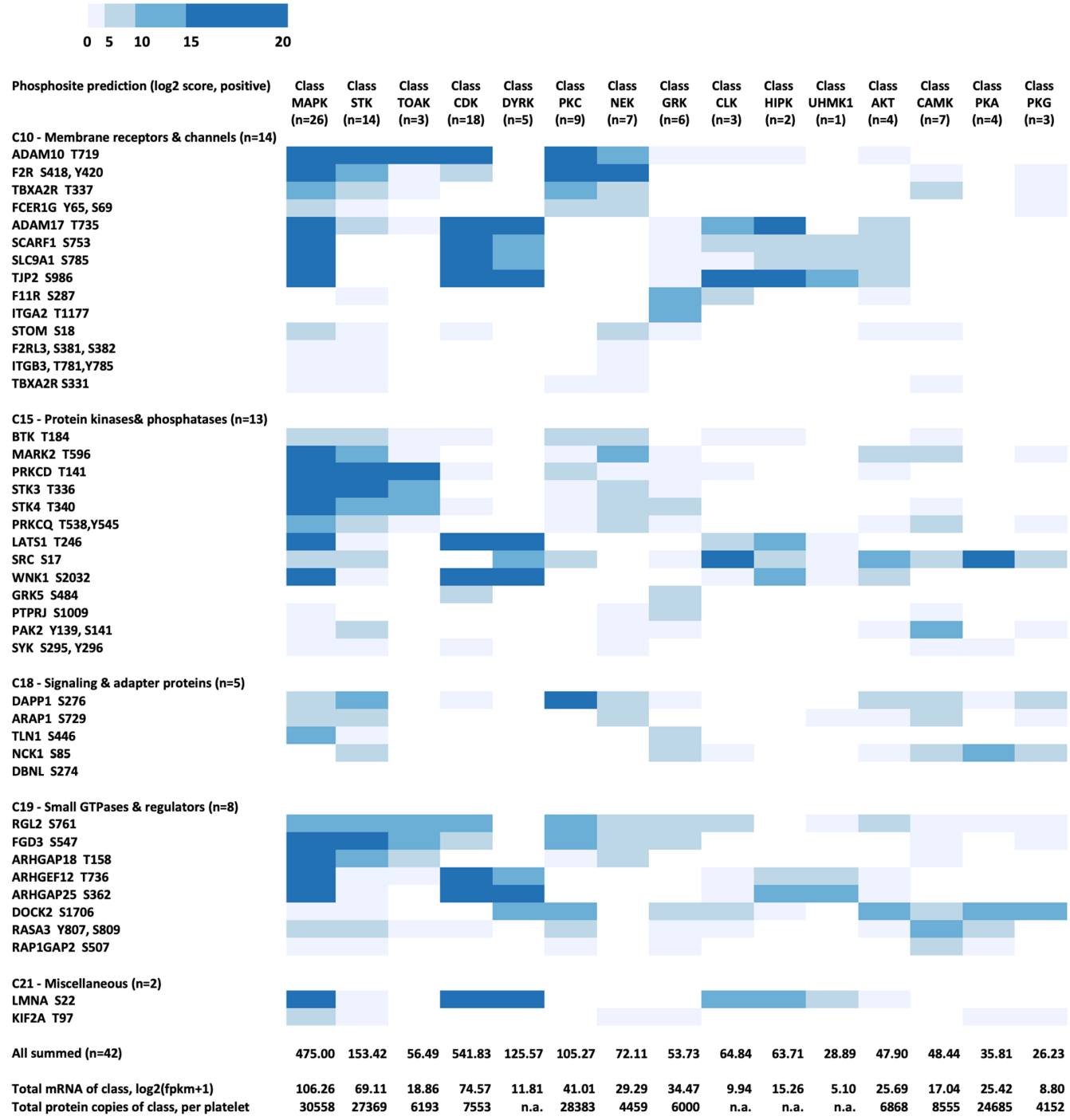

FIGURE 8 Protein kinase assignment of differentially regulated phosphoproteins in platelets exposed to endothelial cells or agonists. Validated phosphopeptides in platelets with differential regulation by endothelial cells or agonists (Table 1) were submitted to the PhosphoSitePlus substrate prediction atlas of 303 serine/threonine kinases. Only kinase classes with 15 highest summative log2 prediction scores (positive) are shown; for complete dataset, see Datafile S1J. Grouping of classes was as follows. *AKT (n = 4)*: AKT1, AKT2, AKT3, GSK3A; *CAMK (n = 7)*: CAMK1, CAMK1D, CAMK2D, CAMK2G, CAMK4, CAMKK1, CAMKK2; *CDK (n = 18)*: CDK1, CDK10, CDK12, CDK13, CDK14, CDK16, CDK17, CDK18, CDK19, CDK2, CDK4, CDK5, CDK6, CDK7, CDK8, CDK9, CDKL1, CDKL5; *CLK (n = 3)*: CLK1, CLK2, CLK3; *DYRK (n = 5)*: DYRK1A, DYRK1B, DYRK2, DYRK3, DYRK4; *GRK (n = 6)*: GRK1, GRK2, GRK3, GRK4, GRK5, GRK7; *HIPK (n = 2)*: HIPK1, HIPK2; *MAPK (n = 26)*: MAPK13, MAPK3, MAPK14, MAPK9, MAPK10, MAPK8, MAPK1, MAP4K3, MAP4K5, MAP3K20, MAP3K1, MAPK7, MAP4K4, MAP3K11, MAP4K1, MAP3K10, MAP3K2, MAP3K3, MAP3K8, MAP3K14, MAP3K6, MAP3K7, MAP3K5, MAP2K5, MAP2K1, MAP2K2; *NEK (n = 7)*: NEK1, NEK11, NEK3, NEK4, NEK6, NEK7, NEK9; *PCKA (n = 4)*: PRKACA, PRKACB, PRKACG1, PRKAA1; *PKG (n = 3)*: PRKG1, PHKG1, PRKG2; *PCK (n = 9)*: PRCKA, PRCKB, PRCKC, PRCKD, PRCKE, PRCKH, PRCKI, PRCKQ, PRCKZ; *STK (n = 14)*: STK10, STK11, STK16, STK17A, STK24, STK25, STK26, STK3, STK32C, STK33, STK38L, STK38, STK39, STK4. *TAOK (n = 3)*: TAOK1, TAOK2, TAOK3; *UHMK1 (n = 1)*: UHMK1. Also indicated are summed, corresponding mRNA and protein copy levels in human platelets.[41]

15306860, 2024, 4, Downloaded from https://faseb.onlinelibrary.wiley.com/doi/10.1096/fj.202300360RR by Test, Wiley Online Library on [12/02/2024]. See the Terms and Conditions (https://onlinelibrary.wiley.com/terms-and-conditions) on Wiley Online Library for rules of use; OA articles are governed by the applicable Creative Commons License

platelet activation or inhibition, namely Rac serine/threonine kinases (AKT), calmodulin-dependent kinases (CAMP), protein kinases A (PKA), and protein kinases G (PKG) showed relatively low predictive scores (Figure 8). These observations are in line with the limited effects of HUVEC-produced mediators' prostacyclin and nitric oxide on platelet activation under flow.

While promising new insights into the interactions of endothelial cells with platelets, our study does have some limitations. First, all experiments were performed with HUVEC at low passage numbers, as a relatively stable source of endothelial cells. However, these cultured human, umbilical vein-derived cells will differ in aspects from the vascular-bed-specific endothelial cells present in a healthy subject. Second, the flow-perfusion experiments and the phospho-proteome analyses indicated no more than minor roles of the endothelial-derived nitric oxide and prostacyclin (acting via PKG and PKA, respectively) in the suppression of platelet adhesion and activation. However, they do not rule out a role of these mediators under in vivo conditions. Our data rather point to the presence of other factors that also regulate the interactions between endothelial cells and platelets, as well as the endothelial-modulated phospho-proteome in platelets. Third, the PhosphoSitePlus analysis points to the likely involvement of poorly studied protein kinase families in platelets. Further studies will need to identify the actual contribution of the respective kinase family members.

Additionally, further research will need to identify which other endothelial cell-derived factors can modify the platelet phosphoproteome and, thereby, regulate platelet inhibition under (patho)physiological conditions. We anticipate that the currently identified 42 differentially regulated serine/threonine phosphosites—operating as a network—may serve as useful biomarkers to disclose such mediators and the corresponding protein kinase signaling pathways in platelets.

AUTHOR CONTRIBUTIONS

Isabella Provenzale, Fiorella A. Solari, Claudia Schönichen, Sanne L. N. Brouns, and Delia I. Fernández designed and performed experiments and analyzed the data. Marijke J. E. Kuijpers, Paola E. J. van der Meijden, Jonathan M. Gibbins, and Albert Sickmann provided funding and supervision. Isabella Provenzale, Chris Jones, and Johan W. M. Heemskerk conceptualized and wrote the manuscript. All authors have read and agreed to the manuscript.

ACKNOWLEDGMENTS

IP and DIF are supported by the European Union's Horizon 2020 research and innovation program under the Marie Sklodowska-Curie grant agreement TAPAs No. 766118, IP is enrolled in a joint PhD program of the Universities of Maastricht (The Netherlands) and Reading (United Kingdom). DIF is enrolled in a joint PhD program of the universities of Maastricht (The Netherlands) and Santiago de Compostela (Spain). CS is supported by the European Union's Horizon 2020 research and innovation program under the Marie Sklodowska-Curie grant agreement TICARDIO No. 813409. CS participates in a joint PhD program of the universities of Maastricht (The Netherlands) and Mainz (Germany).

DISCLOSURES

JWMH is a scientific advisor at Synapse Institute Maastricht. The other authors report no relevant conflicts of interest.

DATA AVAILABILITY STATEMENT

Raw mass spectrometry data and Proteome Discoverer search results are deposited in the ProteomeXchange repository, identifier PXD047399. The remaining data that support the findings of this study are available in the methods and/or supplementary material and datafile of this article.

ORCID

Fiorella A. Solari https://orcid.org/0000-0003-3199-6296
Claudia Schönichen https://orcid.org/0000-0002-4327-5472
Paola E. J. van der Meijden https://orcid.org/0000-0002-6532-2583
Jonathan M. Gibbins https://orcid.org/0000-0002-0372-5352
Albert Sickmann https://orcid.org/0000-0002-2388-5265
Chris Jones https://orcid.org/0000-0001-7537-1509
Johan W. M. Heemskerk https://orcid.org/0000-0002-2848-5121

REFERENCES

1. Van Hinsbergh VW. Endothelium: role in regulation of coagulation and inflammation. *Semin Immunopathol*. 2012;34:93-106.
2. Versteeg HH, Heemskerk JW, Levi M, Reitsma PH. New fundamentals in hemostasis. *Physiol Rev*. 2013;93:327-358.
3. Naseem KM, Roberts W. Nitric oxide at a glance. *Platelets*. 2011;22:148-152.
4. Smolenski A. Novel roles of cAMP/cGMP-dependent signaling in platelets. *J Thromb Haemost*. 2012;10:167-176.
5. Bye AP, Unsworth AJ, Gibbins JM. Platelet signaling: a complex interplay between inhibitory and activatory networks. *J Thromb Haemost*. 2016;14:918-930.
6. Morello S, Caiazzo E, Turiello R, Cicala C. Thromboinflammation: a focus on NTPDase1/CD39. *Cells*. 2021;10:2223.
7. Gagnet C, Brunet A, Pernollet MG, Devynck MA, Astarie-Dequeker C. Endothelin-3, Ca^{2+} mobilization and cyclic GMP content in human platelets. *Eur J Pharmacol*. 1996;310:67-72.

15306860, 2024, 4, Downloaded from https://faseb.onlinelibrary.wiley.com/doi/10.1096/fj.202300360RR by Test, Wiley Online Library on [12/02/2024]. See the Terms and Conditions (https://onlinelibrary.wiley.com/terms-and-conditions) on Wiley Online Library for rules of use; OA articles are governed by the applicable Creative Commons License

8. Zelaya H, Rothmeier AS, Ruf W. Tissue factor at the crossroad of coagulation and cell signaling. *J Thromb Haemost*. 2018;16:1941-1952.
9. Provenzale I, Brouns SLN, van der Meijden PE, Swieringa F, Heemskerk JW. Whole blood based multiparameter assessment of thrombus formation in a standard microfluidic device to proxy in vivo haemostasis and thrombosis. *Micromachines*. 2019;10:e787.
10. Sakurai Y, Hardy ET, Ahn B, et al. A microengineered vascularized bleeding model that integrates the principal components of hemostasis. *Nat Commun*. 2018;9:509.
11. Riddle RB, Jennbacken K, Hansson KM, Harper MT. Endothelial inflammation and neutrophil transmigration are modulated by extracellular matrix composition in an inflammation-on-a-chip model. *Sci Rep*. 2022;12:6855.
12. Brouns S, Provenzale I, van Geffen JP, van der Meijden PE, Heemskerk JW. Localized endothelial-based control of platelet aggregation and coagulation under flow: proof-of-principle vessel-on-a-chip study. *J Thromb Haemost*. 2020;18:931-941.
13. Van der Meijden PE, Heemskerk JW. Platelet biology and functions: new concepts and future clinical perspectives. *Nat Rev Cardiol*. 2019;16:166-179.
14. Fernandez DI, Kuijpers MJ, Heemskerk JW. Platelet calcium signalling by G-protein coupled and ITAM-linked receptors regulating anoctamin-6 and procoagulant activity. *Platelets*. 2021;32:863-871.
15. Swieringa F, Solari FA, Pagel O, et al. Diagnostic potential of phosphoproteome of prostaglandin-treated platelets from patients with confirmed or suspected pseudohypoparathyroidism type 1a linked to platelet functions. *Sci Rep*. 2020;10:11389.
16. Beck F, Geiger J, Gambaryan S, et al. Time-resolved characterization of cAMP/PKA-dependent signaling reveals that platelet inhibition is a concerted process involving multiple signaling pathways. *Blood*. 2014;123:e1-e10.
17. Beck F, Geiger J, Gambaryan S, et al. Temporal quantitative phosphoproteomics of ADP stimulation reveals novel central nodes in platelet activation and inhibition. *Blood*. 2017;129:e1-e12.
18. Makhoul S, Walter E, Pagel O, et al. Effects of the NO/soluble guanylate cyclase/cGMP system on the functions of human platelets. *Nitric Oxide*. 2018;76:71-80.
19. Van Gorp RM, Broers JL, Reutelingsperger CP, Hornstra G, van Dam-Mieras MC, Heemskerk JW. Peroxide-induced membrane blebbing in human endothelial cells associated with glutathione oxidation but not apoptosis. *Am J Phys*. 1999;277:C20-C28.
20. Westein E, van der Meer AD, Kuijpers MJ, Frimat JP, van den Berg A, Heemskerk JW. Atherosclerotic geometries exacerbate pathological thrombus formation poststenosis in a von Willebrand factor-dependent manner. *Proc Natl Acad Sci USA*. 2013;110:1357-1362.
21. Feijge MA, Ansink K, Vanschoonbeek K, Heemskerk JW. Control of platelet activation by cyclic AMP turnover and cyclic nucleotide phosphodiesterase type-3. *Biochem Pharmacol*. 2004;67:1559-1567.
22. Heemskerk JW, Willems GM, Rook MB, Sage SO. Ragged spiking of free calcium in ADP-stimulated human platelets: regulation of puff-like calcium signals in vitro and ex vivo. *J Physiol*. 2001;535:625-635.
23. Fernandez DI, Provenzale I, Cheung HY, et al. Ultra-high throughput Ca^{2+} assay in platelets to distinguish between ITAM-linked and G-protein coupled receptor activation. *iScience*. 2022;25:103718.
24. Navarro S, Stegner D, Nieswandt B, Heemskerk JW, Kuijpers ME. Temporal roles of platelet and coagulation pathways in collagen and tissue factor induced thrombus formation. *Int J Mol Sci*. 2021;23:358.
25. De Witt SM, Swieringa F, Cavill R, et al. Identification of platelet function defects by multi-parameter assessment of thrombus formation. *Nat Commun*. 2014;5:4257.
26. Auger JM, Kuijpers MJ, Senis YA, Watson SP, Heemskerk JW. Adhesion of human and mouse platelets to collagen under shear: a unifying model. *FASEB J*. 2005;19:825-827.
27. Brouns S, van Geffen JP, Campello E, et al. Platelet-primed interactions of coagulation and anticoagulation pathways in flow-dependent thrombus formation. *Sci Rep*. 2020;10:11910.
28. Munnix IC, Strehl A, Kuijpers MJ, et al. The glycoprotein VI-phospholipase Cγ2 signaling pathway controls thrombus formation induced by collagen and tissue factor in vitro and in vivo. *Arterioscler Thromb Vasc Biol*. 2005;25:2673-2678.
29. Jooss NJ, De Simone I, Provenzale I, et al. Role of platelet glycoprotein VI and tyrosine kinase Syk in thrombus formation on collagen-like surfaces. *Int J Mol Sci*. 2019;20:e2788.
30. Solari FA, Mattheij NJ, Burkhart JM, et al. Combined quantification of the global proteome, phosphoproteome, and proteolytic cleavage to characterize altered platelet functions in the human Scott syndrome. *Mol Cell Proteomics*. 2016;15:3154-3169.
31. Hogrebe A, von Stechow L, Bekker-Jensen DB, Weinert BT, Kelstrup CD, Olsen JV. Benchmarking common quantification strategies for large-scale phosphoproteomics. *Nat Commun*. 2018;9:1045.
32. Post H, Penning R, Fitzpatrick MA, et al. Robust, sensitive, and automated phosphopeptide enrichment optimized for low sample amounts applied to primary hippocampal neurons. *J Proteome Res*. 2017;16:728-737.
33. De Graaf EL, Giansanti P, Altelaar AF, Heck AJ. Single-step enrichment by Ti^{4+}-IMAC and label-free quantitation enables in-depth monitoring of phosphorylation dynamics with high reproducibility and temporal resolution. *Mol Cell Proteomics*. 2014;13:2426-2434.
34. Solari FA, Dell'Aica M, Sickmann A, Zahedi RP. Why phosphoproteomics is still a challenge. *Mol BioSyst*. 2015;11:1487-1493.
35. Yu SH, Ferretti D, Schessner JP, Rudolph JD, Borner GH, Cox J. Expanding the Perseus software for omics data analysis with custom plugins. *Curr Protoc Bioinformatics*. 2020;71:e105.
36. Szklarczyk D, Gable AL, Lyon D, et al. STRING v11: protein-protein association networks with increased coverage, supporting functional discovery in genome-wide experimental datasets. *Nucleic Acids Res*. 2019;47:D607-D613.
37. Casado P, Rodriguez-Prados JC, Cosulich SC, et al. Kinase-substrate enrichment analysis provides insights into the heterogeneity of signaling pathway activation in leukemia cells. *Sci Signal*. 2013;6:rs6.
38. Wiredja DD, Koyutürk M, Chance MR. The KSEA App: a web-based tool for kinase activity inference from quantitative phosphoproteomics. *Bioinformatics*. 2017;33:3489-3491.
39. Hornbeck PV, Kornhauser JM, Latham V, et al. 15 years of PhosphoSitePlus: integrating post-translationally

15306860, 2024, 4, Downloaded from https://faseb.onlinelibrary.wiley.com/doi/10.1096/fj.202300360RR by Test, Wiley Online Library on [12/02/2024]. See the Terms and Conditions (https://onlinelibrary.wiley.com/terms-and-conditions) on Wiley Online Library for rules of use; OA articles are governed by the applicable Creative Commons License

modified sites, disease variants and isoforms. *Nucleic Acids Res*. 2019;47:D433-D441.
40. Johnson JL, Yaron TM, Hunstman EM, et al. An atlas of substrate specificities for the human serine/threonine kinome. *Nature*. 2023;613:749-766.
41. Huang J, Swieringa F, Solari FA, et al. Assessment of a complete and classified platelet proteome from genome-wide transcripts of human platelets and megakaryocytes covering platelet functions. *Sci Rep*. 2021;11:12358.
42. Van Geffen JP, Brouns S, Batista J, et al. High-throughput elucidation of thrombus formation reveals sources of platelet function variability. *Haematologica*. 2019;104:1256-1267.
43. Gillespie M, Jassal B, Stephan R, et al. The reactome pathway knowledgebase 2022. *Nucleic Acids Res*. 2022;50:D687-D692.
44. Hornbeck PV, Zhang B, Murray B, Kornhauser JM, Latham V, Skrzypek E. PhosphoSitePlus, 2014: mutations, PTMs and recalibrations. *Nucleic Acids Res*. 2015;43:D512-D520.
45. Coppin L, Najimi M, Bodart J, et al. Clinical protocol to prevent thrombogenic effect of liver-derived mesenchymal cells for cell-based therapies. *Cells*. 2019;8:846.
46. Huang J, Zhang P, Solari FA, et al. Molecular proteomics and signalling of human platelets in health and disease. *Int J Mol Sci*. 2021;22:9860.
47. Saklatvala J, Rawlinson L, Waller RJ, et al. Role for p38 mitogen-activated protein kinase in platelet aggregation caused by collagen or a thromboxane analogue. *J Biol Chem*. 1996;271:6586-6589.
48. Yacoub D, Théorêt JF, Villeneuve L, et al. Essential role of protein kinase C delta in platelet signaling, αIIbβ3 activation, and thromboxane A_2 release. *J Biol Chem*. 2006;281:30024-30035.

SUPPORTING INFORMATION

Additional supporting information can be found online in the Supporting Information section at the end of this article.

How to cite this article: Provenzale I, Solari FA, Schönichen C, et al. Endothelium-mediated regulation of platelet activation: Involvement of multiple protein kinases. *The FASEB Journal*. 2024;38:e23468. doi:10.1096/fj.202300360RR

15306860, 2024, 4, Downloaded from https://faseb.onlinelibrary.wiley.com/doi/10.1096/fj.202300360RR by Test, Wiley Online Library on [12/02/2024]. See the Terms and Conditions (https://onlinelibrary.wiley.com/terms-and-conditions) on Wiley Online Library for rules of use; OA articles are governed by the applicable Creative Commons License